Petrophysical Controls on Effective Thermal Conductivity Estimates

Thesis submitted in accordance with the requirements of the University of Adelaide for an Honours Degree in Geophysics

Alicia Pollett

November 2015

THE UNIVERSITY of ADELAIDE

PETROPHYSICAL CONTROLS ON EFFECTIVE THERMAL CONDUCTIVITY ESTIMATES

PETROPHYSICAL CONTROLS ON THERMAL CONDUCTIVITY

ABSTRACT

This study focuses on the Thermal Optical Scanner devised by Popov (used for thermal conductivity estimates) and whether this method should use more than one type of means calculation when using individual measurements made upon a core sample to produce a single mean, representative thermal conductivity for the sample. The study stems from the well-known theory that different means can be used to calculate the mean thermal conductivity for variations in grain and bedding orientations exhibited by varying lithologies and investigates whether the use of different means can result in more physically accurate and representative thermal conductivity averages for various lithologies. Through the analysis of the individual measurements made upon each of the samples, the arithmetic, geometric and harmonic means were calculated to determine whether a significant difference could be observed between the three means. The largest difference observed was 0.19W/mK^{-1}, which was considered to not substantiate a significant enough difference between the means to make recommendations of changes to how the computer program associated with the scanner calculates the final mean thermal conductivity output. As this analysis included the measurement of thermal conductivity upon 85 samples across three drill holes from central Southern Australia, the study also investigates the links between particular petrophysical characteristics including porosity and grain size and the exhibited thermal conductivities of these samples. The strongest correlation was observed between porosity and dry thermal conductivity, where porosities greater than 10% (total sample volume) resulted in evident decreases in exhibited thermal conductivity. No correlation was determined between average grain size and the standard deviation of the thermal conductivity and they also displayed no correlation with thermal conductivity measurements.

KEYWORDS

Thermal Conductivity, Thermal Optical Scanner, Petrophysics

TABLE OF CONTENTS

LIST OF FIGURES

LIST OF TABLES

INTRODUCTION

Thermal conductivity is the ability of a material to transport heat and is a fundamental property of rocks required to determine heat flow (Decker & Walsh, 1966). There are three main methods used to the measure this property in rock samples including the divided bar apparatus, the line-source method and the thermal optical scanner; this paper focuses on the Thermal Optical Scanner devised by Yuri Popov in 1983 (Popov, 1983). Advantages of the thermal optical scanner over other methods include its speed of operation, its ability to measure variation of thermal conductivity along samples; it is a contactless form of measurement and it allows for the measurement of cylindrical surfaces (common in core samples). The scanner makes measurements of thermal conductivity approximately every 1mm along a sample using a heat source to heat the sample, along with hot and cold sensors that also scan along the sample, giving the arithmetic mean of the thermal conductivity measurements as output. The program associated with the scanner (named TCS) calculates this average thermal conductivity by taking the arithmetic mean of the numerous individual measurements made upon the rock samples.

Thermal anisotropy is an important physical property to consider when calculating the average thermal conductivity of a sample. Particular rocks are highly thermally anisotropic, meaning that the value of thermal conductivity will change depending on the direction in which it is measured. This is particularly prevalent within lithologies such as Shale, which are present within the following data set. Mineralogy of a rock will influence its anisotropy, along with the fabric and bedding planes of the rock (Davis et al., 2007). A thermally anisotropic mineral will conduct thermal energy

differently along different axes of its crystals and if these minerals are in abundance within a sample in a preferred orientation, it will present as thermally anisotropic. Therefore, if a sample's thermal conductivity is measured along different axes, it may be observed to exhibit varying thermal conductivities, which needs to be taken into account when considering which measurement best represents in-situ conditions of heat flow.

There are three typical types of mathematic means used to characterise an average for a set of data – arithmetic, geometric and harmonic means. It is well established that for layered media (perpendicular to its bedding/foliation), the most effective average is the harmonic mean (Beardsmore & Cull, 2001). As the scanner is set to calculate the thermal conductivity using an arithmetic mean, this paper will investigate the variations in the mean thermal conductivity observed between each of the different means and whether the variations between them are significant enough to suggest that layered lithologies use a harmonic mean for thermal conductivity calculation. As the scanner will measure thermal conductivity for a variety of lithologies, the arithmetic mean will most likely not be the most suitable for all rock types, typically when rocks are layered and measurements are taken orthogonal to these layers (for example, Shales).

The measurements made upon samples for the use of investigating the variance in means will also be used to analyse any observable correlations between a number of petrophysical characteristics and thermal conductivity. Core samples from three drill holes in central South Australia are used to make these measurements, all of which present a variety of lithologies with a majority of sedimentary samples as well as a few

igneous samples; from which links between their petrophysical characteristics (porosity, grain size etc.) and thermal conductivity can be made.

If significant variance exists between the means (calculated from thermal conductivity measurements for particular lithologies), then we may be able to make recommendations to improve the final estimate of thermal conductivity made by the Thermal Optical Scanner program. Recommendations would then be made to suggest that the program associated with the scanner is able to calculate the harmonic or geometric mean at the user's discretion when the operator determines it would be best suited for the lithology being scanned.

If it is determined that a mean other than the arithmetic mean is most suitable for the calculation of thermal conductivity, recommendations would allow for a more physically accurate output of the effective thermal conductivity and hence determination of heat flow (for which these measurements are used). As the geometry of rock samples vary in layering and grain orientation as well as in sample orientations during measurement, it may be necessary to alter the averaging method used on the sample being measured. The goal of this study is to determine the magnitude of systematic error that may arise from an inappropriate averaging scheme and make recommendations about the conditions under which a different form of averaging than the default should be used.

BACKGROUND

THERMAL CONDUCTIVITY

Thermal conductivity is a physical property that requires a thorough understanding when attempting to model the heat flow of a region. The method used for measurement of thermal conductivity needs to be understood to ensure that one of the major components required for the calculation of heat flow is accurate. The following study will examine the way in which thermal conductivity is measured using the Thermal Optical Scanner, the way thermal conductivity varies with changes in petrophysical properties of rocks and how these factors can contribute to heat flow estimates.

Thermal conductivity is a measure of how rocks and their constituent minerals are able to conduct thermal energy. Every mineral exhibits a range of average thermal conductivities, which allows for an estimate of the thermal conductivity range of a rock sample, dependent upon the constituent minerals present. Figure 1 demonstrates the range of thermal conductivities for a set of common rock types, which can be used to give an approximation of the thermal conductivity that is to be expected when a particular lithology is its measured. For example, Quartz exhibits one of the highest thermal conductivities of all minerals and therefore we can expect a Quartzite to have a relatively high average thermal conductivity (5.0 WmK^{-1}) (Vasseur et al., 1992) (Pribnow & Umsonst, 1993).

The value of thermal conductivity that is measured for a rock sample is attributed to many factors including the mineral composition of the rock, the porosity, the pore fluid and the anisotropic properties of the minerals within the rocks (Brigaud & Vasseur,

1989). Physical properties including burial depth can have an influence on the thermal conductivity exhibited by a sample, dependent upon its lithology; mudstones and sandstones have been shown to display the strongest relationship to burial depth and thermal conductivity (Liu et al., 2011).

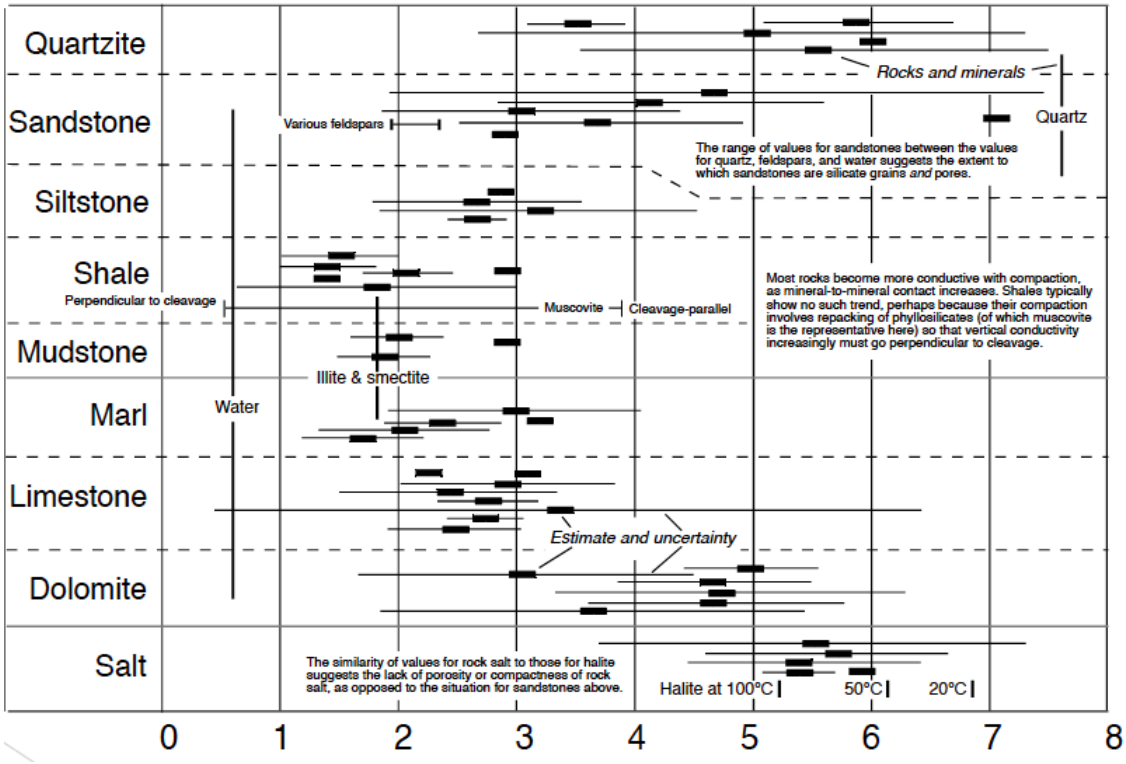

Figure 1: The expected range of thermal conductivity values for a common set of sedimentary rocks. (Modified from Beardsmore & Cull, 2001)

THERMAL OPTICAL SCANNER

There are three leading methods of measuring thermal conductivity of rock samples: The divided bar method, the thermal optical scanner and the line-source method. Studies conducted after numerous measurements made with each of the three devices show that all methods give consistent results and that each device would be most suitable for specific situations but state that the optical scanner is the most efficient device of the three and that it is able to provide measurement on both plane and cylindrical surfaces without any severe constraints for sample size and quality of surface

treatment (Popov et al., 1998). A more in depth explanation of the optical scanner can be found in Popov et al (1999).

Clauser & Huenges (1995) produced a review of the thermal conductivity for a set of crustal rocks and concluded that a single value of thermal conductivity could not be assigned to any rock type as thermal conductivity may vary by as much as a factor of 2-3 for any given rock type. Therefore, it needs to be ensured that thermal conductivity is correctly measured to allow for an accurate estimate of heat flow. Through thermal conductivity measurements made on samples from three drill cores within the same region in central South Australia, the study will focus on the way thermal conductivity changes with varying petrophysical characteristics of the rocks, the associations between factors such as porosity and average grain size of rocks and the variance recorded by the optical scanner.

THERMAL CONDUCTIVITY AND PETROPHYSICAL CHARACTERISTICS

The links between particular petrophysical characteristics and thermal conductivity are well studied. The following study continues to focus on the possible controls that properties including grain size, rock type (and therefore mineralogy) and porosity have on the effective thermal conductivity.

The effect of porosity on thermal conductivity has been extensively studied (Blackwell & Steele, 1989) (Midttømme et al., 1998). Similar to the following study, thermal conductivity measurements have been made upon sets of sedimentary samples and it has commonly been concluded that porosity is the main control on the thermal conductivity exhibited by the rock. The thermal conductivity of sedimentary rocks

generally increases with depth through the effect of compaction (Beardsmore & Cull, 2001), allowing for heat to flow through the lithology along a pathway of least resistance (where pore space is minimized).

Studies suggest that grain size can have an effect on thermal conductivity; however this is only proven true when quartz is the dominant mineral and contributes to more than 49% of the overall mineral composition of the rock (Jessop 1990). Therefore, it should be stated that for a particular dominant mineralogy within a given sample, larger grain size could lead to an observed larger thermal conductivity. With samples that have average larger grain sizes, it is also hypothesised that the thermal conductivity measurements will have a corresponding effect on the value of variance that is observed in the data. Given that this study is being conducted on a machine that is not yet widely distributed, no studies were found to have investigated the effect on the value of variance observed by the device.

We expect a linear relationship between dry and saturated thermal conductivity measurements but also expect saturated samples to exhibit marginally greater thermal conductivities due to the greater thermal conductivity of water compared to air (Beardsmore & Cull, 2001) and would therefore see a linear relationship that is greater than a 1:1 relationship. Studies show that with increasing porosity of the rock the difference in dry and saturated thermal conductivity will become larger (Jessop, 1990), however considering that as porosity increases the thermal conductivity overall will become larger for both the dry and saturated states, both measurements will increase and therefore a linear trend should be observed.

CALCULATION OF MEAN THERMAL CONDUCTIVITY

The optical scanner is designed to calculate the thermal conductivity using the arithmetic mean (equation 1.1) of each of the individual thermal conductivities measured along a sample to give a final representative thermal conductivity for the sample. However, since a harmonic mean is more physically correct orthogonal to horizontally layered strata, a harmonic mean is more appropriate in a general for drill core. The calculated thermal conductivity in the following study is representative of the vertical thermal conductivity in-situ, in which heat flows vertically to the surface. However if using drill core samples, the orientation of the drill hole needs to be accounted for when determining the direction of the heat flow for each measured sample.

An arithmetic mean is effective for rocks that have random grain alignments within their bedding/foliation, which describes the geometry of most sedimentary lithologies (even after burial and compaction); however for Shale lithologies, their sheet silicate grains will rotate to a preferred horizontal alignment once they are buried and compacted (Bennett et al., 1981); alternating layers of quartz sand and clay or as in a gneiss, alternating micaceous and quartz/feldspar foliation will also present rotated grain orientations which are most effectively calculated using a harmonic mean. With regards to shale lithologies (which are most prevalent within the following data set), conductivity with depth will remain constant or decrease, instead of increase - which is observed for all other sedimentary sequences. In this case, it is well established that for layered media (such as Shale), the most effective mean to apply in the calculation of thermal conductivity is a harmonic mean (Beardsmore & Cull, 2001) (equation 1.2).

The three means are defined as:

Arithmetic Mean: $$\lambda_B = \sum_{i=1}^{n} z_i \lambda_i \quad (1.1)$$

Harmonic Mean: $$\frac{1}{\lambda_B} = \frac{1}{Z} \sum_{i=1}^{n} \frac{z_i}{\lambda_i} \quad (1.2)$$

Geometric Mean: $$\lambda_B = \prod_{i=1}^{n} \lambda_i^{z_i} \quad (1.3)$$

where for each of the equations, λ_B represents the average thermal conductivity, λ_i represents each measurement and n represents the number of measurements within the sequence. For the weight applied to the arithmetic mean (vertical bedding), z_i represents the thickness of the ith bed and λ_i represents the thermal conductivity of the ith bed. For the harmonic mean (horizontal bedding), Z represents the total horizontal bed thickness; z_i represents the thickness of the ith horizontal layer and λ_i represents the thermal conductivity of the ith horizontal layer. For the geometric mean (random orientation), $\lambda_i^{z_i}$ represents the thermal conductivity of a single grain to the power of its fractional proportion (constituent volume). Refer to figure 2 for a diagrammatic expression of each of the means in terms of thermal conductivity calculation.

This study will determine if the harmonic mean is the most effective way to calculate an estimate of thermal conductivity for layered lithologies. The variation in physical characteristics between different rock types may prove the need for a change in the mathematics behind which the TCS program associated with the scanner calculates thermal conductivity. A sample that consists of predominantly shale will have a thin, repeating layered structure whereas a quartzite will have a well-rounded, randomly aligned grain structure (figure 2a & 2c, respectively); it is essential to determine if calculating the thermal conductivity using a mean other than the arithmetic mean may give a more accurate result.

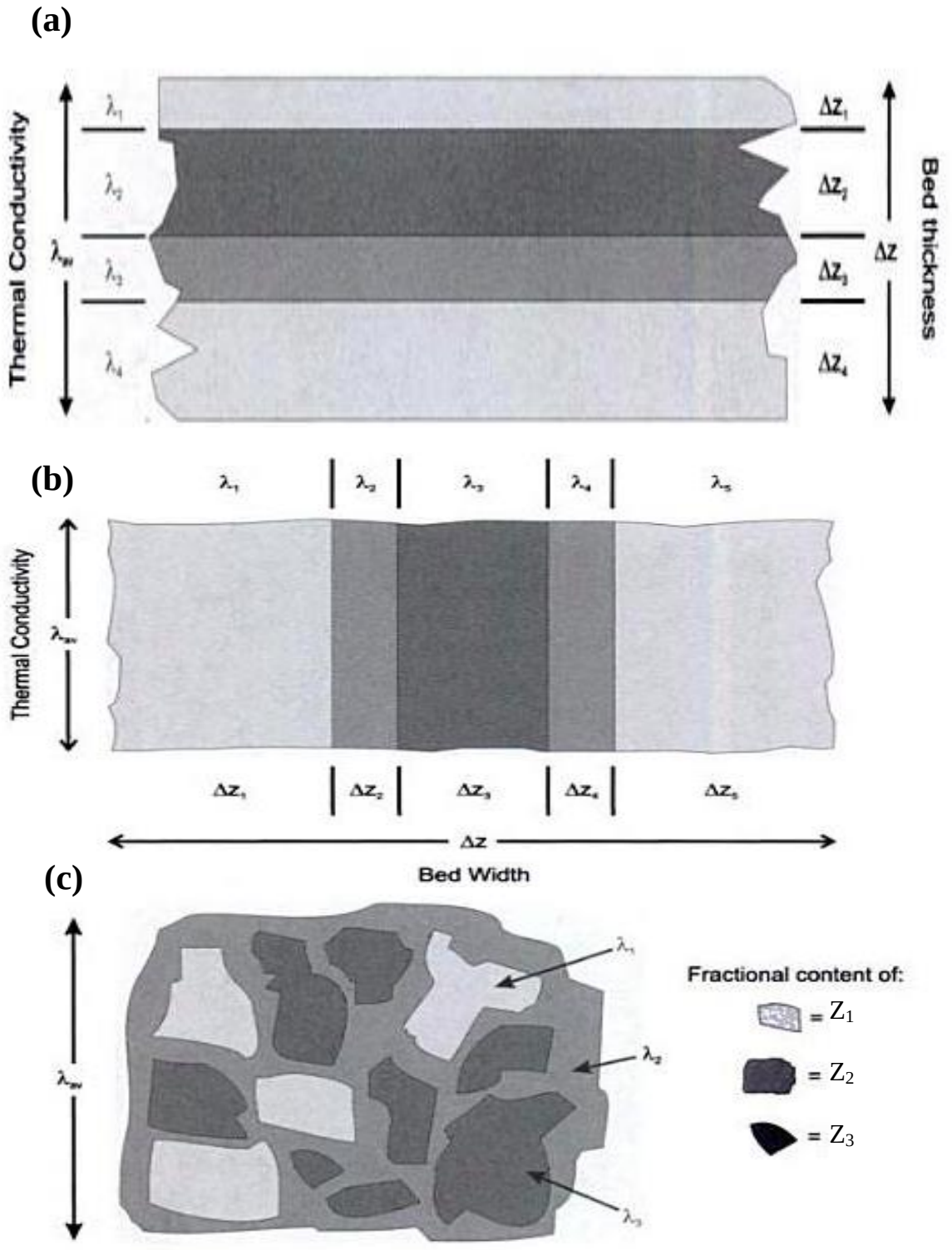

Figure 2: Conceptual model of in-situ conditions and components (for thermal conductivity calculation) and hence the most suitable means for these in-situ conditions (a) a harmonic mean, (b) an arithmetic mean and (c) a geometric mean (Modified from Beardsmore & Cull, 2001)

METHODS

Core samples were collected from three drill holes located in central southern Australia approximately 170km Northwest of Port Augusta that were drilled by Monax Mining Limited. Samples of core were chosen from the entire selection of drill core and were selected to contain a representative range of lithologies and features observed within the core. In total, 85 pieces of core were selected from the three holes, which represent nine lithologies including predominantly sedimentary and some igneous samples.

Before thermal conductivity measurements are conducted upon samples, each sample is photographed twice (once dry and once wet) and can then be used for visual reference. Following photography, the first measurement made upon the core is the specific gravity, which involves measuring the mass of the core sample once in air and once again when submerged in water. The two measurements of mass are then repeated once the sample has been saturated in water within a vacuum for a minimum of four hours. When both measurements of mass have been recorded, the following equation is used to determine the porosity of the sample:

$$Porosity = \left(\frac{Mass\ of\ Saturated\ Core\ in\ Air - Mass\ of\ Unsaturated\ Core\ in\ Air}{Mass\ of\ Saturated\ Core\ in\ Water - Mass\ of\ Unsaturated\ Core\ in\ Water}\right)\ x\ 100 \qquad (2.1)$$

Once porosity is calculated, a strip along the samples (approximately 2cm wide) is painted or taped black (paint is the most practical option if the core sample contains loose sediment grains; tape if effective if the sample has a relatively smooth surface to attach the tape to) to ensure homogeneous absorption from the heat source on the thermal optical scanner (Jorand et al., 2013).

Once the sample has been prepared, it is placed upon the thermal optical scanner between two standards (the first with expected lower thermal conductivity of the sample and the second with an expected higher thermal conductivity). The scanner is then started and a heat source moves along a track beneath the sample, with a cold and hot sensor located both before and after the heat source.

When the scanner has completed its pass along the sample and the second standard, it is stopped and the data is sent to the accompanying computer program to give the output measurements. It is at this point that the operator is required to choose what individual measurements along the core sample are used in the thermal conductivity calculation. Commonly, the measurements made at the ends of samples are disregarded, as they are known to be inaccurate due to rough edges of core samples (figure 3). Once the measurement range has been selected, the program will produce an output with a single representative thermal conductivity of the sample. This output is calculated by collecting the thermal conductivity measurements taken within the operator's chosen range (scanner takes measurements every 1mm along the scanning line) and calculates the arithmetic mean of these measurements to produce a single, representative thermal conductivity for the sample. A more in depth outline of the thermal optical scanning process is given in the Appendix.

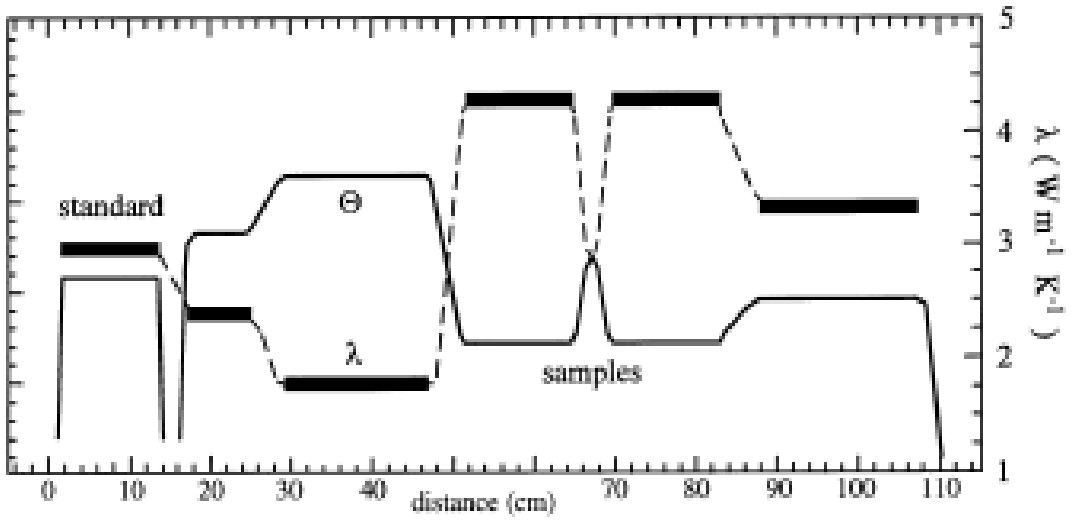

Figure 3: Schematic of the output received from the thermal optical scanner once it has completed measurements of the sample/s and the two standards. It is at this stage of output that the operator can constrain the range of thermal conductivity measurements used for the final calculation. (Modified from Popov et al., 1999)

The measurement of thermal conductivity on the optical scanner is completed twice for each sample – once when the sample is dry and then repeated once again when the sample has been saturated in water in a vacuum for a minimum of four hours. In a given day of measurements, a number of samples are chosen at random to re-measure (once they have returned to room temperature from the first measurement) to ensure that no instrument drift is occurring. Refer to Popov et al (1999) for a detailed discussion of the mechanics and process of how the thermal optical scanner measures and produces thermal conductivity output for samples. Once porosity and thermal conductivity measurements have been made, the data is entered into Matlab and excel for analysis. It is through these programs that the variance of the measurements can also be calculated.

OBSERVATIONS AND RESULTS

Initially, histograms of individual thermal conductivity measurements for each sample were produced to display the distribution of the measurements for each of the 85 samples (refer to appendix). The samples showed a variation in spreads for each of the samples, including spreads that reasonably resembled Gaussian distributions, spreads that displayed positive and negative skews and also spreads the were greatly uneven. BHDD01 samples were determined to have the smallest range of spreads, whereas several samples within PHDD1202 and SDDD01 showed large spreads of >2 W/mK^{-1} (figure 4). Skarn and Mafic Dyke (Dolerite) lithologies tend to correlate with samples displaying uneven spreads.

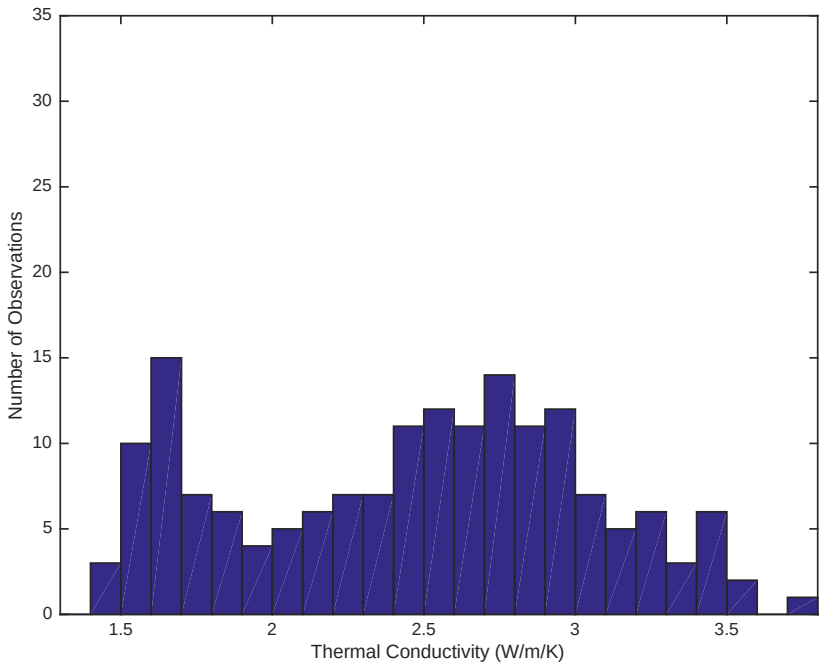

Figure 4: A histogram representing the range of measured thermal conductivities for sample PHDD1202-05 (Skarn). Note the large spread of thermal conductivity measurements along with the large number of observations for a single sample (172 measurements).

These histograms allowed for particular samples with uneven spreads to be analysed in more detail, including plotting each of the individual thermal conductivity measurements made upon a single sample. BHDD01-08 - a sandstone sample, was the only sample in the BHDD01 hole to display a distinctly uneven spread, which can be correlated with the wide range of values for individual measurements made upon the sample (figure 5). The contrast between uneven spreads and Gaussian, uniform spreads can be observed between figures 5 & 6; figure 6 displays the individual thermal conductivity measurements along the sample BHDD01-35, a sample of sandstone which displayed a reasonably Gaussian distribution of conductivity – the value of individual measurement variations, although relatively fluctuating, are evidently smaller than that of BHDD01-08 (note the smaller range on the x-axis in figure 6 – BHDD01-35 – and the much larger x-axis range in figure 5 – BHDD01-08).

The largest variations in means (although not considered large enough to be significant) were observed in samples located within the holes PHDD1202 and SDDD01. Sample SDDD01-22 (Mafic Dyke - Dolerite) showed a difference of 0.19 W/mK^{-1} between the arithmetic and harmonic means; when observing figure 7 (SDDD01-22), it should be noted that this sample has the largest spread of individual thermal conductivity measurements (note the large range on the x-axis – $3.5W/mK^{-1}$). Sample PHDD1202-05 (Skarn) displayed a difference of 0.147 W/mK^{-1} between the arithmetic and harmonic means; when observing the histogram of the sample's spread (figure 4), it is clear that not only was the range of measured thermal conductivities large, but the volume of measurements of this sample was one of the largest of the entire data set (172 measurements upon one piece of core).

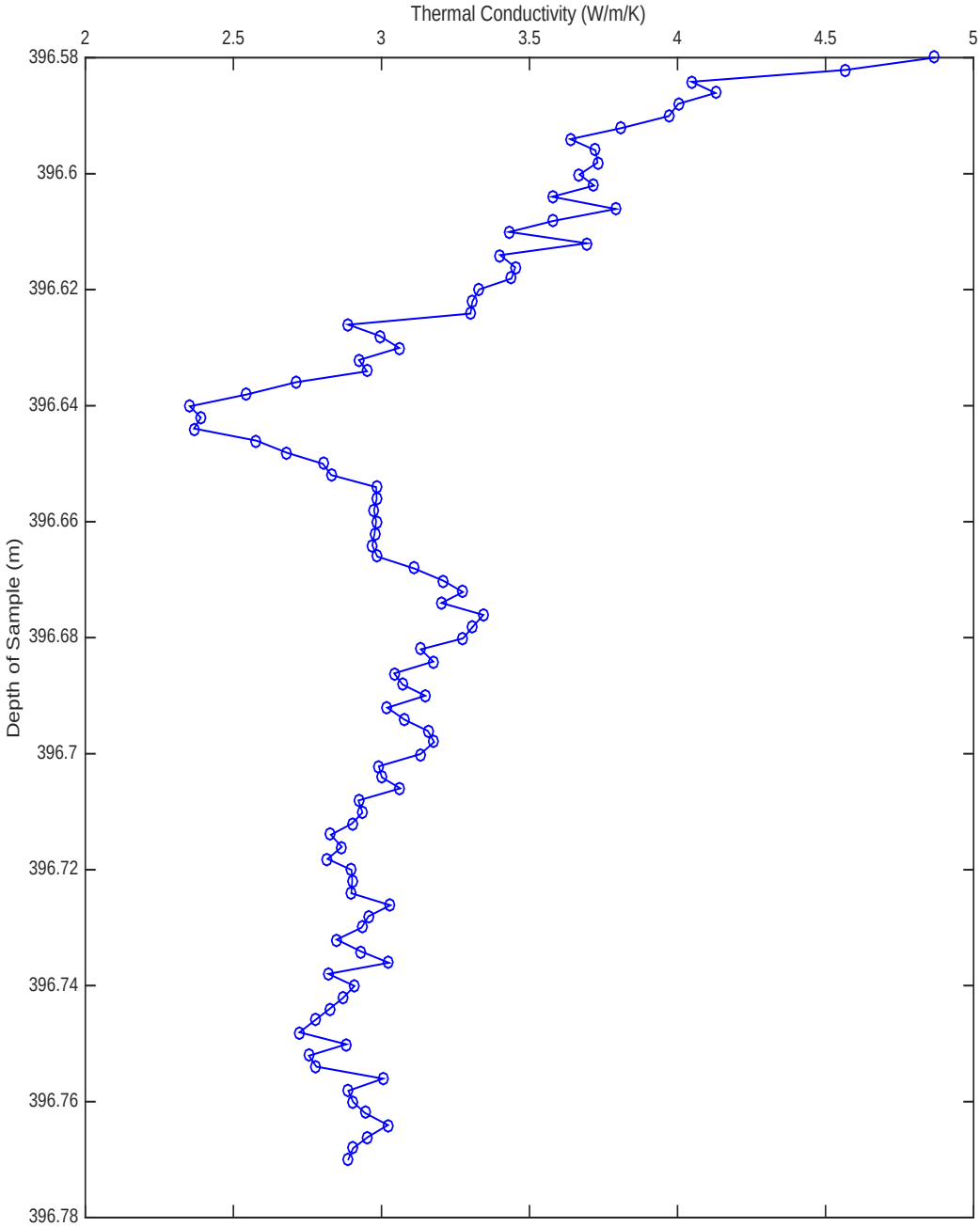

Figure 5: Depth/Thermal Conductivity Profile for Sample BHDD01-08. Note the appearance of smooth transitions between each of the thermal conductivity measurements with no large fluctuations; however also note the larger range of thermal conductivities over the entire sample (2.3 – 4.9 W/mK^{-1})

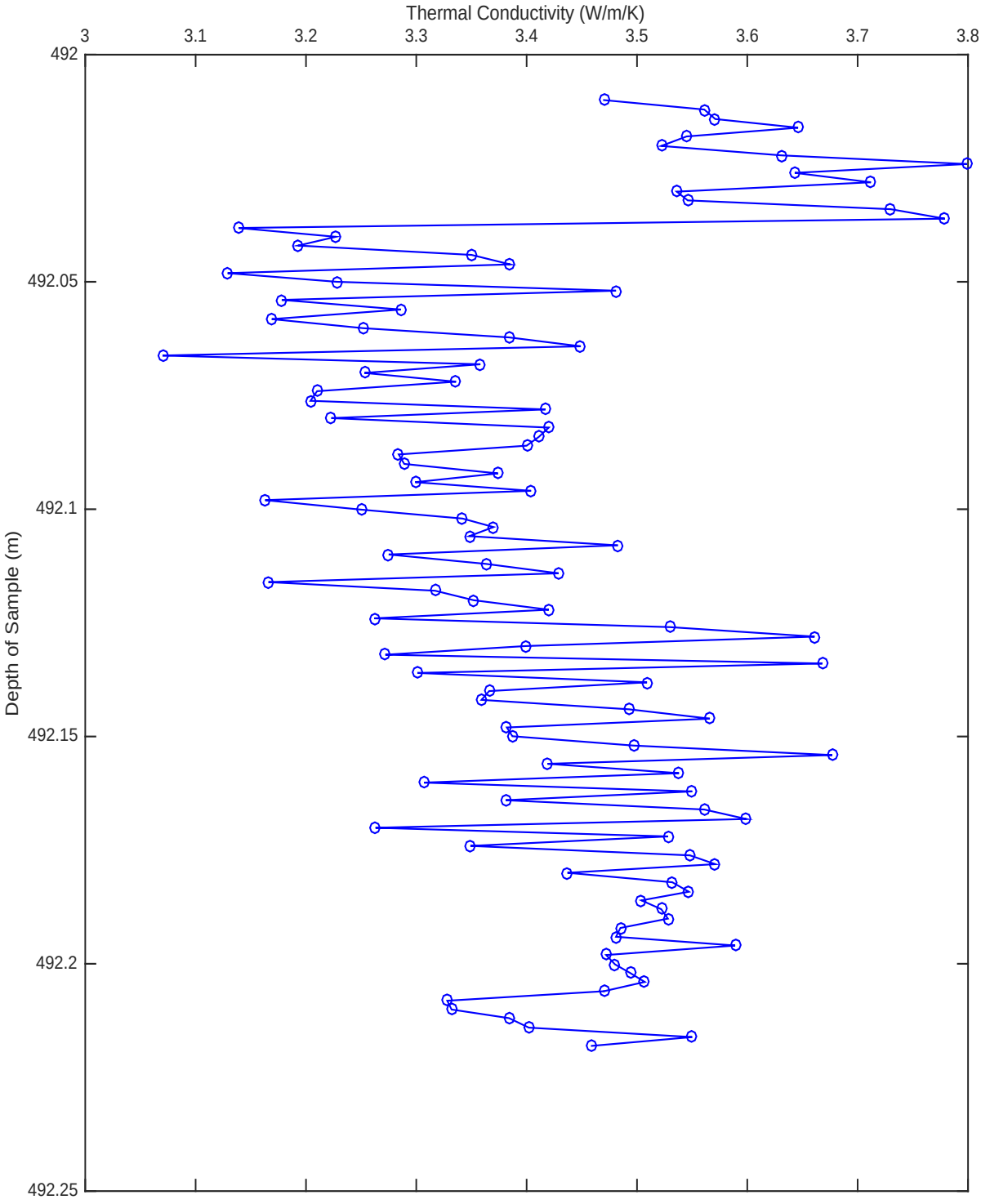

Figure 6: Depth/Thermal Conductivity Profile for Sample BHDD01-35. Note the large fluctuations in thermal conductivities measurements along the core; however also note the small range of thermal conductivities over the entire sample, only 3.0 – 3.8 W/mK^{-1}

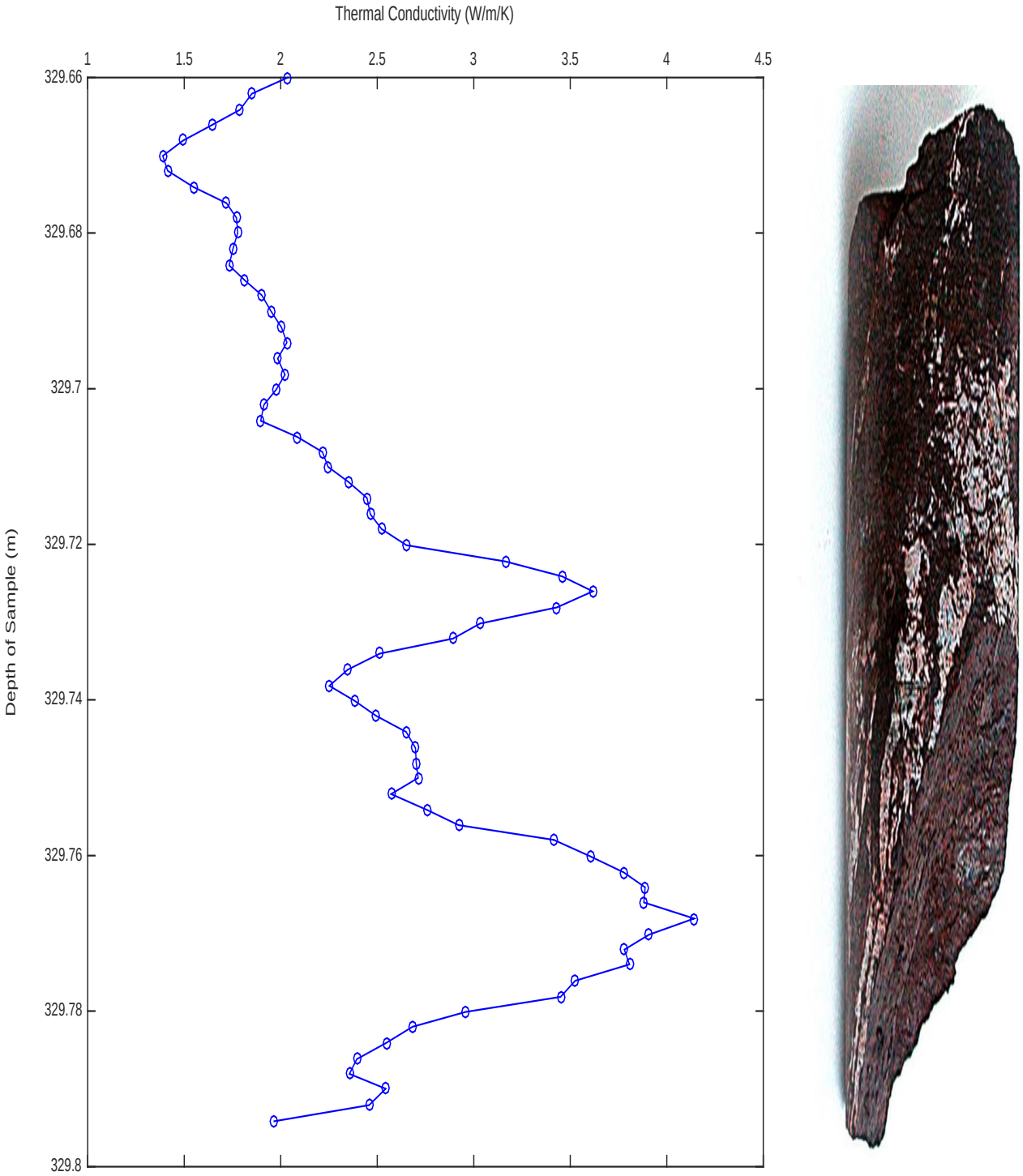

Figure 7: Depth/Thermal Conductivity Profile of Sample SDDD01-22 alongside the photograph of the dry sample. Note the smooth transitions between measurements but the large range of thermal conductivities exhibited by the sample (1.4 – 4.3W/mK^{-1}), which is important to note considering the small size of the sample (<15cm). Note also the evidence of fluid pathways within the sample, indicated by the white markings on the core.

All sample measurements were analysed for correlations between several petrophysical characteristics including thermal conductivity & porosity, grain size & variance and variance & grain size. Correlations were observed for saturated and dry conductivity (figure 9) and weak correlations were observed for porosity & thermal conductivity (figure 8) as well as a possible correlation between average grain size & the variance of the measurement (figure 11).

Measurement results show that mean thermal conductivity within the samples range from 2.303 W/mK^{-1} to 4.324 W/mK^{-1} with an average dry thermal conductivity measurement of 3.277 ± 0.626 W/mK^{-1}. As is also presented in Table 1, Skarn samples represent those that exhibited some of the lowest average thermal conductivities (2.303 W/mK^{-1}), while conglomerate samples included those with some of the highest average thermal conductivities (4.414W/mK^{-1}). The maximum mean thermal conductivity value was measured on a sandstone (sample BHDD01-19) from the BHDD01 hole (4.482 W/mK^{-1}). The largest range of conductivities was observed for sandstones, with a mean thermal conductivity range of 2.167 W/mK^{-1}; this also corresponds to the largest number of measurements recorded any of the lithologies (n=39). Clastic rocks account for those samples that exhibited thermal conductivities above 4.0 W/mK^{-1}, whereas igneous lithologies accounted for a large range of thermal conductivities (2.798 – 4.043 W/mK^{-1}) that were on average lower than sedimentary samples.

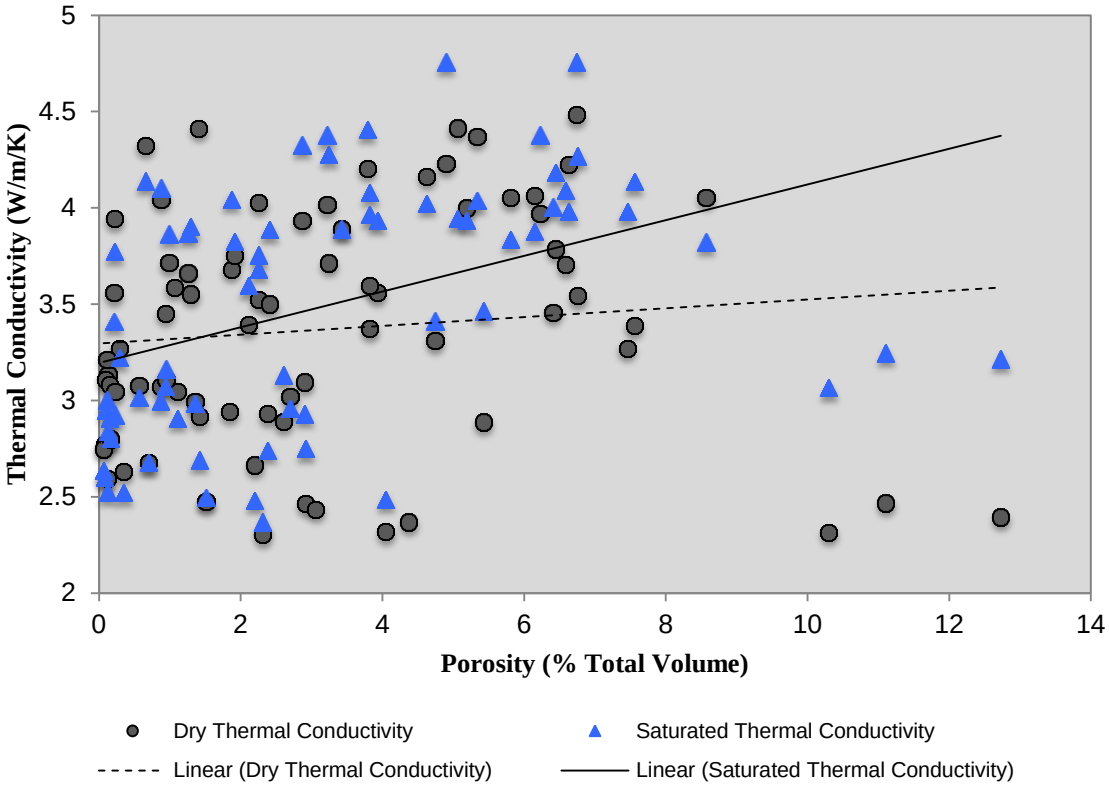

Figure 8: The relationship between measured dry and saturated thermal conductivity of samples and their porosity. Note at porosities >10%, there appears to be a stronger distinction between dry and saturated thermal conductivities and that the trend changes to show lower thermal conductivities at higher porosities.

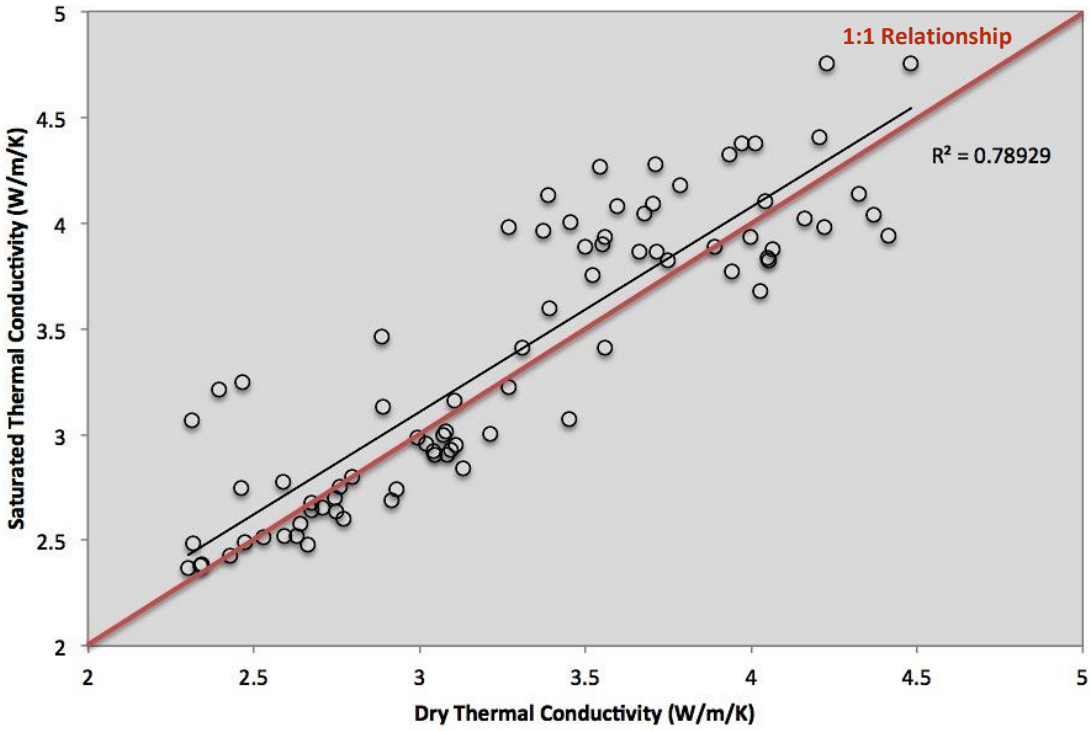

Figure 9: The relationship between dry and saturated thermal conductivity measurements. There is an observable correlation between the two variables, with saturated samples exhibiting generally higher thermal conductivities. The red line demonstrates what trend line the data would centre on, if the two variables exhibited a 1:1 relationship.

The effect of porosity on the thermal conductivity is shown to differ depending upon the state of the sample – dry or saturated. Dry thermal conductivity is observed to show no strong correlation with increasing porosity; however when the samples are saturated, the measured thermal conductivity is observed to increase with increasing porosity (figure 8). It can also be observed that with porosities greater than 10% total volume, there appears to be a clear decrease in both dry and saturated thermal conductivity. Interestingly, when the dry and saturated thermal conductivity measurements are plotted against each other (figure 9), we observe a reasonably strong positive linear relationship which indicates that saturating the samples had an only minimal effect on changing the observed thermal conductivity, which appears to be disputed in figure 8 at higher porosities, where there is a clearly a distinct difference in the thermal conductivities between dry and saturated samples.

The effect of average grain size within samples has no observable correlation with measured thermal conductivity (figure 10) and at best a weak positive correlation. There is possibly a weak influence observable on the standard deviation of measurements dependent upon grain size (figure 11), while an increase in porosity results in an observable decrease in standard deviation of measurements. It should be noted that although this decrease is observable, most standard deviations remain within 2-10% of the mean measured thermal conductivity for each measurement (represent by the blue rectangle in figure 12).

The calculated arithmetic, geometric and harmonic means for each of the samples indicate that there is no significant difference observed between the means for each of

the samples (refer to appendix for individual sample calculations). Table 2 demonstrates the largest difference in means observed from all samples is 0.19 W/mK^{-1}, which is a deviation too small to be categorized as significant.

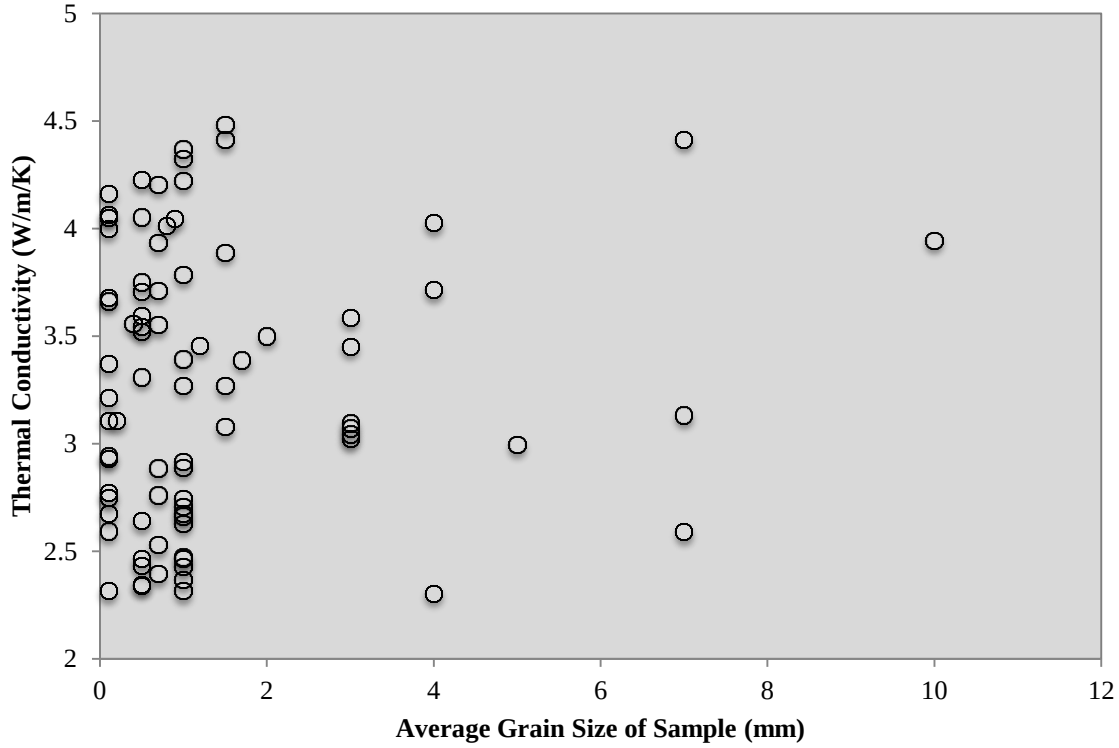

Figure 10: The relationship between the measured dry thermal conductivity of samples and their average grain size.

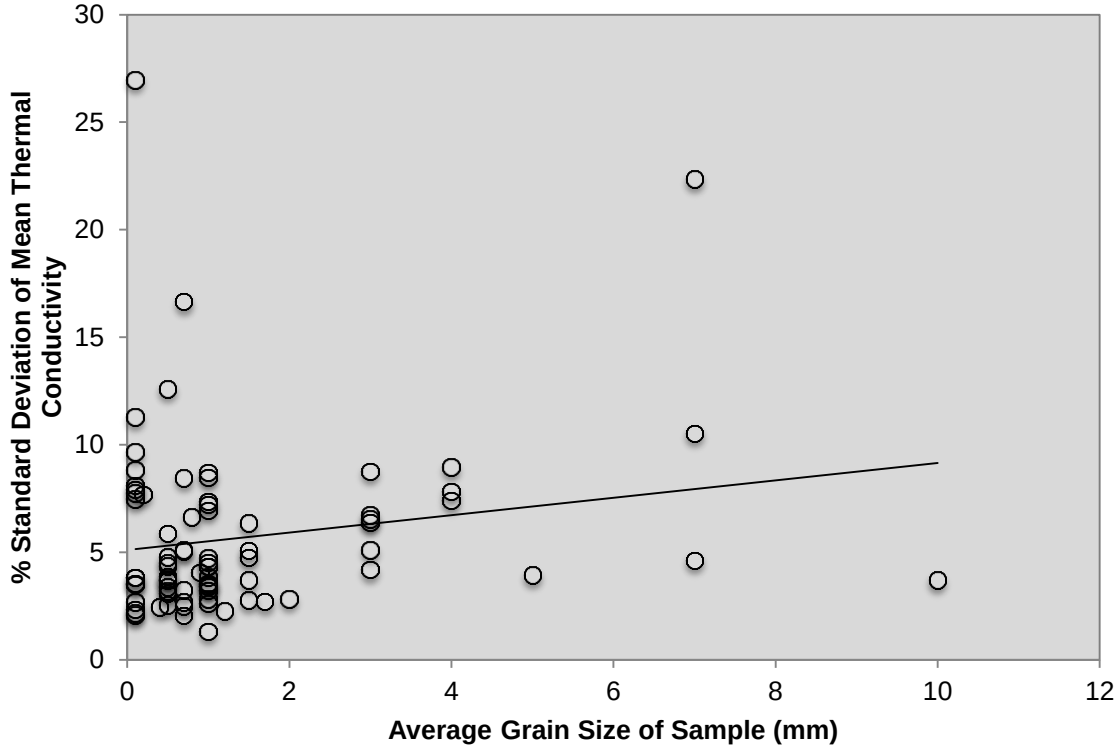

Figure 11: The relationship between the standard deviation (represented as the proportion of the mean thermal conductivity) and the average grain size of the sample

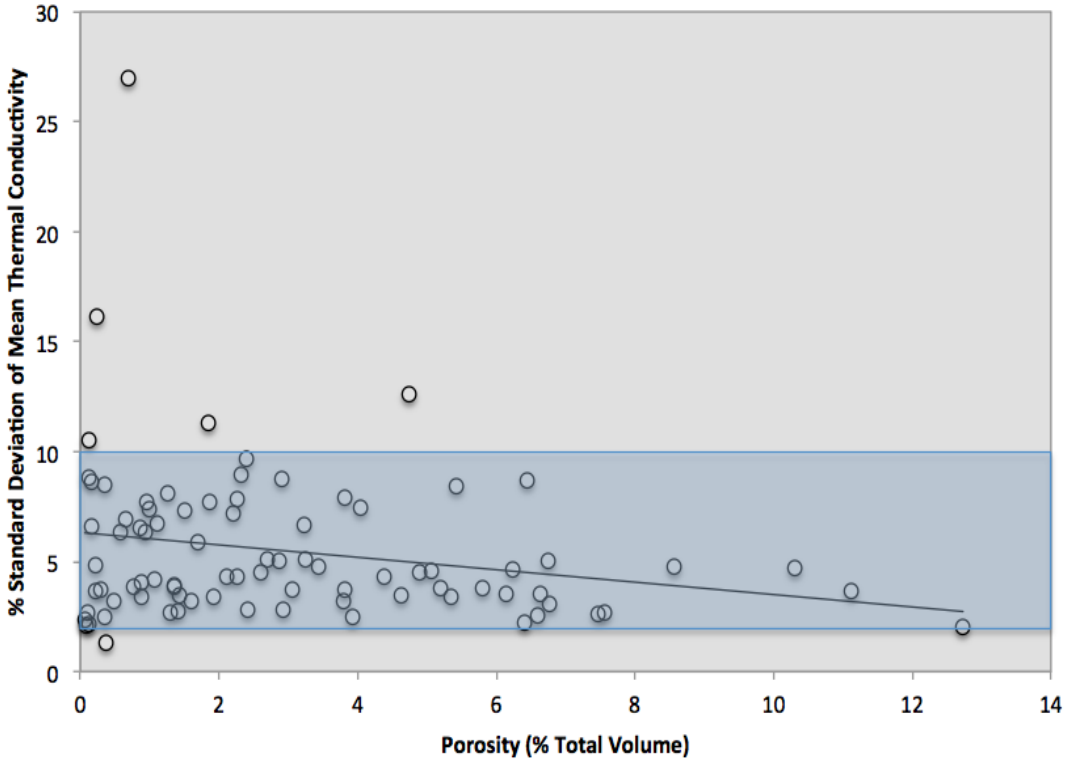

Figure 12: The relationship between the standard deviation (represented as the proportion of the mean thermal conductivity) and the porosity of the sample. The blue region represents that regardless of porosity, most measurements have a value of variance ranging between 2-10% of the mean thermal conductivity.

Lithology:	Number of Samples	Thermal Conductivity Range (W/mK^{-1})	Mean ± S.D. (W/mK^{-1})
Conglomerate	2	3.94 – 4.41	4.17
Mudstone	2	4.10 – 4.32	4.16
Shale	8	3.37 – 4.16	3.88±0.27
Pegmatite	1	3.55	3.55
Gawler Range Volcanics	6	2.47 – 4.04	3.50±0.65
Sandstone	39	2.31 – 4.48	3.36±0.60
Granite	5	2.79 – 3.21	3.05±0.15
Mafic Dyke (Dolerite)	9	2.31 – 3.71	2.86±0.39
Skarn	**13**	**2.30 – 3.10**	**2.60±0.22**

Table 1: Thermal Conductivity of the sample set of lithologies from central South Australia ranked by mean conductivity

Sample Number:	Lithology:	Arithmetic Mean (W/mK^{-1})	Variation from Harmonic Mean (W/mK^{-1})	Variation from Geometric Mean (W/mK^{-1})
BHDD01 – 08	Sandstone	3.313	0.05	0.02
BHDD01 – 22	Sandstone	3.581	0.04	0.02
PHDD1202 – 05	Skarn	2.464	0.14	0.07
PHDD1202 – 08	Skarn	2.623	0.07	0.03
SDDD01 – 22	Dolerite	2.531	0.19	0.09

Table 2: Thermal conductivity of samples as calculated by an arithmetic mean and the difference observed between the arithmetic value and the value calculated by both harmonic and geometric means. Samples chosen represent the largest deviation in values between the three means evident within the set of samples.

DISCUSSION

Results from calculations of harmonic and geometric means, when compared to the arithmetic means of thermal conductivity calculated by the optical scanner program show no significant difference between the means (table 2). Each of the calculated means (arithmetic, harmonic and geometric) are not the same, however the largest difference observed between means was sample SDDD01-22, whose difference was only 0.190 W/mK^{-1}; a deviation too small to be classified as significant enough to consider a change in the way the program calculates the mean thermal conductivity for a sample.

The idea for this study was based upon the well-known theory about means calculation, which suggests that the use of an arithmetic mean for the calculation of an average, representative thermal conductivity for all rock types would not result in accurate and physically representative results given by TCS. Considering that we are aware of the largely varying grain orientations of different rock types and the knowledge that different grain orientations require the calculation of thermal conductivity through the application of different means, this study was undertaken in the expectation that we could determine whether the use of just one mean for all varieties of grain orientations would result in in accurate and physically representative outputs by the program.

By using a random number sequence in Matlab we can calculate whether the arithmetic, geometric and harmonic means vary significantly between randomly generated number sequences. It can be shown that neither uniform nor skewed spreads of randomly generated data will result in a significant difference in the value of the means for the set of data. Considering the well-known theory that the mean of physical properties with layered media should be calculated using a harmonic mean (Beardsmore & Cull, 2001), it was still important to test whether the data sets of the measured thermal conductivity of the samples followed this theory or followed the same principal as when calculating means for randomly generated data sets. The samples listed in table 2 with the greatest differences in means do not correspond to any of the shale samples and therefore it appears that the layered samples do not display a variance between the calculated arithmetic and harmonic means significant enough to recommend that any changes be made to the thermal optical scanning program (TCS).

Interestingly, the variation of the thermal conductivity for the arithmetic and harmonic mean is on average approximately double the value for the variation for the arithmetic and geometric mean (observe in 3rd and 4th columns of table 2). There is no apparent explanation for this trend, as each of the samples that provided the greatest variation in means were from different holes, their lithologies varied and the length of samples greatly varied meaning that there were no consistencies or links that may explain the trend observed between the variance of the means.

Histograms of each core sample's thermal conductivity measurements were produced to give insight into the spread of the individual measurements made upon each piece of core. These histograms showed that few samples exhibited uniform or Gaussian spreads, indicating that for a range of lithologies, thermal conductivity within a single lithology can be relatively variable; which is why the appropriate means calculation needs to be in place to calculate an accurate, representative mean thermal conductivity for each sample.

Depth/Thermal Conductivity plots were produced to give a clear insight into the possible variations and fluctuations in thermal conductivity that can be exhibited by a single sample of core, between 15 and 40cm long. The use of the core photographs allowed for any visible cause of the fluctuations to be identified, as in figure 7, where the gradual movement to higher thermal conductivity measurements could be correlated to the presence of fluid pathways evident as white alteration observed on the core sample. Some samples show smooth transitions between individual thermal conductivity measurements, however still exhibit large ranges of overall conductivity

measured within the sample (figures 5 & 7). While other samples exhibit what appear to be highly fluctuating individual measurements but within smaller conductivity ranges (figure 6). This again stresses the importance of the theory that the appropriate mean is used to calculate the mean thermal conductivity of each sample even though we now understand that the means differ insignificantly.

When analysing results to determine if any petrophysical properties have a control on the thermal conductivity exhibited by the samples, it is clear the only property that appears to have a strong control is porosity. It is well studied and documented that porosity contributes one of the major controls on the thermal conductivity exhibited by rocks, in that an increase in porosity of a sample will result in a decrease of the thermal conductivity; it is clear the results from this data set support this. The porosity and corresponding thermal conductivities shown in figure 8 clearly display that although the data set shows trends of increasing thermal conductivity with increasing porosity, at porosities of 10% total volume and greater, thermal conductivities display a large decrease in value.

The way measured thermal conductivity changes as a function of porosity depends upon the state in which the sample is measured; whether it is dry or saturated with water. We observe that on average, the thermal conductivity exhibited by saturated samples is higher than the thermal conductivity exhibited by dry samples (figure 9). This is to be expected, as the thermal conductivity of water (0.6 W/mK^{-1}) is greater than the thermal conductivity of air (0.023 W/mK^{-1})(Jessop, 1990) and we should therefore observe samples whose pores are filled with a more conductive fluid to exhibit a slightly

increased overall thermal conductivity. This also corresponds to the reason we observe that at porosities of greater than 10% total volume, the thermal conductivity decreases; if a significant proportion of the sample is filled with air or water in its pores (which are low thermal conductors compared to minerals), rather than this space being occupied by greater thermally conductive minerals, we should expect the overall thermal conductivity exhibited by that sample to be lower than other samples who have less pore space filled by these fluids and have more of their total volume occupied by minerals.

Another petrophysical control that was analysed is the average grain size of the samples and observable affects it may have had upon the exhibited thermal conductivity of the sample and the standard deviation of the measurement. There appears to be no strong correlations between the average grain size and the exhibited thermal conductivity of samples and a weak positive correlation between average grain size and standard deviation can be observed.

The way in which average grain size may have any control over the thermal conductivity of samples is strongly dependent upon the mineralogy of samples. Consider two samples that exhibit larger than average grain sizes (for example >1cm) but one sample is abundant in quartz and the other in feldspar, we expect that there will be substantial difference between the thermal conductivities exhibited by the two samples, considering the difference in thermal conductivities of each of the dominant minerals (Quartz = 7.69W/mK^{-1} & Feldspar = 2.34W/mK^{-1})(Beardsmore & Cull, 2001). In the case of this data set, the samples were predominantly sedimentary with an

abundance of quartz present (refer to appendix for logging of core samples) and there is no substantial evidence that grain size has any control over the exhibited thermal conductivity.

There appears to be no strong correlation between the average grain size and the standard deviation of the measurement made upon the sample (figure 11) and any weak positive correlation observed needs to be treated with care as there are clearly some outlying data points within the set that could be influencing the overall trend. It should be noted that the outlying data points within figure 11 are from samples of Skarn, which were observed to give large spreads of thermal conductivity measurements and hence resulted in large standard deviations of measurements. Therefore with Skarn samples commonly exhibiting generally lower thermal conductivities, the standard deviation was likely to represent a larger percentage of the mean thermal conductivity measured; which explains the outlying nature of particular data points in figure 11 - not due to the average grain size.

Although no strong correlation is observed between porosity and the standard deviation of the measurements made upon the samples, it should be noted that the blue rectangle in figure 12 demonstrates that the majority of measurements had standard deviations that fall between 2-10% of the mean thermal conductivity of the sample. This indicates that although the overall error of the scanner is quoted at $\pm 3\%$, each sample's individual measurements can generally be expected to have an uncertainty between 2-10%.

The average thermal conductivities for each rock type fall within the expected documented ranges (for example those quoted in figure 1). Due to the observed quartz content of sandstone samples, it was expected that this rock type may have exhibited a slightly higher average thermal conductivity than was observed; however, this rock type had the largest number of samples of all rock types in the data set and was therefore shown to have the biggest range. It is likely the most accurate average thermal conductivity represented in table 1, as some other rock types have not been sampled amply to produce accurate and representative mean thermal conductivities and ranges – particularly the pegmatite, conglomerate and mudstone samples. All rock types were still included in the data set considering that rock type didn't have a major influence over the petrophysical properties that have been the focus of this study.

A limitation of this study is the inability to test the effect of thermal anisotropy upon the samples. It is a factor that needs to be taken in account when measuring the thermal conductivity of samples as it can result in changing thermal conductivities with changing axes of the samples, however within this study the sample measurements had already taken place and samples were returned before this aspect of measurement could be investigated for this study. It should be noted that other studies have confirmed that thermal anisotropy has a significant effect on the petrophysical characteristics of sedimentary rocks (Popov et al., 2003) which indicates the possibility that if this set of samples were measured on the axis perpendicular to the surface measured for this study, our results could differ– particularly for strongly thermal anisotropic lithologies such as shale.

Further studies include the broadening of the thermal conductivity data set of central South Australian lithological samples including increasing the numbers of samples for each lithology to enable accurate representations of the conductivities for each rock type. A larger thermal conductivity data set can aid in the more accurate estimate heat flow within these regions. With further measurements it should be ensured that thermal conductivity is measured on 2-3 perpendicular axes to account for and investigate any effects of thermal anisotropy.

CONCLUSIONS

Calculations were undertaken to compute the variations in arithmetic, harmonic and geometric means of the thermal conductivity measurements made by the thermal optical scanner; it was determined that there was no significant variation observed between the means to substantiate a recommendation that the way in which the computer program computes mean thermal conductivity be changed.

Thermal conductivity was measured on a total of 85 samples, including 9 different lithologies of sedimentary and igneous rocks. Thermal conductivity ranged from 2.30 W/mK^{-1} measured in Skarn samples to 4.48W/mK^{-1} measured on a Sandstone sample. This range is typical of common sedimentary and igneous rocks and no anomalous conductivities were measured in the data set.

Of the petrophysical characteristics examined, grain size, porosity and standard deviation; porosity appears to have a strong, observable control upon the exhibited thermal conductivity. With porosities greater than 10% total volume of the sample, the thermal conductivity was observed to drop significantly below the trending thermal conductivities of porosities less than 10% total volume. Other petrophysical characteristics were determined to show little to no correlation with thermal conductivity or the standard deviation of thermal conductivity measurements.

ACKNOWLEDGMENTS

I would like to acknowledge the following people, companies and research groups for their support throughout the year. Derrick Hasterok, Martin Hand, Betina Bendall and Alex Musson - thank you for your personal ongoing support and encouragement throughout the past year. I would also like to thank Rian Pate for his assistance with core sample measurement and also to Monax Mining Limited who supplied me with South Australian core samples to undertake this project with. And finally thank you to the South Australian Centre for Geothermal Energy Research (SACGER) for their assistance and encouragement with the project.

REFERENCES

BEARDSMORE, G. R. & CULL, J. P. 2001. C*rustal Heat Flow: A Guide to Measurement and Modelling.* Cambridge University Press, Melbourne, Australia.

BENNETT, R. H., BRYANT, W. R. & KELLAR, H. G. 1981. Clay fabric of selected submarine sediments: Fundamental properties and models, *Journal of Sedimentary Petrology,* **51**, 217-32.

BLACKWELL, D. D. & STEELE, J. L. 1989. T*hermal conductivity of sedimentary rocks: Measurement and Significance.* Springer-Verlag, New York.

BRIGUARD, F. & VASSEUR, G. 1989. Mineralogy, porosity and fluid control on thermal conductivity of sedimentary rocks, *Geophysical Journal,* **98**, 525-542.

CLAUSER, C. & HUENGES, E. 1995. *Thermal Conductivity of Rocks and Minerals.* American Geophysical Union, United States.

DAVIS, M. G., CHAPMAN, D. S., VAN WAGONER, T. M., & ARMSTRONG, P. A. 2007. Thermal conductivity anisotropy of metasedimentary and igenous rocks, *Journal of Geophysical Research,* **112**, 5216 - 5223.

JESSOP, A. M. 1990. *Developments in Solid Earth Geophysics.* Elsevier, Amsterdam.

JORAND, R., VOGT, C., MARQUART, G. & CLAUSER, C. 2013. Effective thermal conductivity of heterogenous rocks from laboratory experiemtns and numerical modeling, *Journal of Geophysical Research: Solid Earth,* **118**, 5225 - 5235.

LIU S., FENG, C., WANG, L. & LI, C. 2011. Measurement and Analysis of Thermal Conductivity of Rocks in the Tarim Basin, Northwest China, *Acta Geologica Sinicia (English Edition),* **85**, 598 - 609.

MIDTTØMME, K., ROALDSET, E. & AAGAARD, P. 1998. Thermal conductivity of selected claystones and mudstone from England, *Clay Minerals,* **33**, 131-145.

POPOV, Y. A., BEREZIN, V. V., SEMENOV, V. G. & KOROSTELEV, V. M. 1985. Complex Detailed Investigations of the Thermal Propoerties of Rocks on the Basis of a Moving Point Source, *Izvestya, Earth Physics,* **21**, 64 - 70.

POPOV Y. A., PRIBNOW, D. F., SASS, J.H., WILLIAMS, F. W. & BURKHARDT, H. 1999. Characterization of rock thermal conductivity by high-resolution optical scanning, *Geothermics,* **28**, 253-276.

POPOV, Y., TERTYCHNYI, V., ROUMISHKEVICH, R., KOROBKOV, D. & POHL, J. 2003. Interrelations Between Thermal Conductivity and Other Physical Poroperties of Rocks: Experimental Data, *Pure and Applied Geophsyics,* **160**, 1137 - 1161.

PRIBNOW, D. & UMSONST, T. 1993. Estimation of thermal conductivity from the mineral composition: Influence of fabric and anisotropy, *Geophysical Research Letters,* **20**, 2199-2202.

VASSEUR, G., BRIGAUD, F. & DEMONGODIN, L. 1992. Thermal conductivity estimation in sedimentary basins, *Tectonophysics,* **244**, 167-174.

WALSH, J. B. & DECKER, E. R. 1966. Effect of Pressure and Saturating Fluid on the Thermal Conductivity of Compact Rock, *Journal of Geophysical Research,* **71**, 3053 - 3061.

APPENDIX:

The following is a detailed procedure for the use of the Thermal Optical Scanner from BOWKER, C. 2013, ***TCS Optical Scanner – Operating Procedure***, for the South Australian Centre for Geothermal Energy Research (SACGER), The University of Adelaide

Setup of the Scanner and TCS:

1. Ensure that all cables from the optical scanning machine are plugged in to the device and the computer. It is important to ensure that the **DAQ** and **Stepper Cables** are plugged into the **correct COM port** on your computer (COM port means USB port in this context). It is also vital that the drivers for the **Serial to USB converter cables** are installed. The TCS software needs to be told which COM port each cable is plugged into.
2. Turn the power on at the wall socket, and then switch on the power button at the rear of the electronic supply unit. A red light will come on indicating the machine has been switched on.
3. On the main toolbar, click **Setup > Measurement Parameters**. The Setup window will appear as shown below. Here you can change the device from 'TC only' to 'TC and TD' mode if desired, by clicking the appropriate radar button. It will be necessary to shut down and restart the program if you do this.
4. If purely measuring thermal conductivity, the select the 'TC only' option. If you require the measurement of thermal diffusivity, select the 'TC and TD' option.
5. It is necessary to tell the software which reference standards are going to be used during the measurement. The greatest accuracy will be achieved when the thermal conductivity of the sample and the reference standards is a close as possible (so repeated measurements may be necessary if the sample TC is unknown). To do this, on the main toolbar select **Standards > Edit used standards**
6. The standards can be changed by either clicking on one of the radar buttons on the left hand side of the window under **Standard set**, or each standard can be changed manually using the drop down menus below **Standard 1** and **Standard 2** respectively. It is recommended that only the pre-determined standard sets be used for 'TC only' measurements.
7. Close the **Standards** window. A prompt will appear asking 'Set recommended heat source power?'. Selecting **OK** will ensure that the power level for the heat source is set to the recommended level for the standards selected.
8. This procedure should be followed at the beginning of every measurement session to ensure the parameters are set correctly.
9. It is important to adjust the temperature sensors before **every measurement**, to ensure that any changes in room temperature are taken into account by the software. On the main toolbar, click **Sensors > Sensor Adjustment**
10. Take a reference standard, which is **not going to be used** in the subsequent measurement. It is important to ensure that heat input is minimised from sources such as the optical scanner or your hands (i.e. do not handle it for more time than is necessary). It should be representative of the ambient room temperature. Various reference standards are kept beneath the optical scanner in a metal briefcase and cover the ranges of thermal conductivities that will be measured in samples.

11. Click **Start** on the 'adjust sensors' window. Follow the prompts that appear on the screen. You will need to place your temperature reference standards first over the 'Hot' sensor (i.e. the sensor behind the heat source, relative to the direction of travel of the optical head). Do not touch the scanner or the standard whilst the adjustment is taking place.
12. The prompts will then ask you to move the standard to the 'Cold' sensor. Repeat as per the 'Hot' sensor. You should have two 'bumpy' lines appear on the 'Sensor Temperatures' window.

Sample placement and measurement:

13. It is very important to ensure your samples are arranged correctly on the scanner stage before a measurement is started. You can simultaneously measure as many samples as you wish, provided they fit on the stage with the reference standards.
14. Place one of the appropriate reference standards at the beginning of the red taped section of the scanner stage. **All standards and samples must be placed with the black taped surfaces facing downward.** Check that the black tape is aligned with the aperture by looking underneath the stage with a torch.
15. Place your samples on the stage in a logical order. Place the second reference standard after the samples. **If there is not enough space on the red tape to fit all your samples and reference standards, then you will need to remove one of your samples to make space**.
16. If samples are saturated, ensure to dry them with a cloth to ensure that no water drips onto the machine. Also ensure that the tape is still securely attached after wiping down.
17. You can measure samples with flat surfaces OR cylindrical surfaces, as shown in Figure 7. N.B. cylindrical surfaces **need to be propped** with the metal core props, so that they are coincident with the top of the scanner stage. If measuring cylindrical surfaces, you will also need to **apply correction factors** to the results (in your spreadsheet after the measurement has been performed), as there is a systematic error incurred as a result of doing this instead of measuring a flat surface.

Collecting thermal data:

18. If all of the previous instructions have been followed correctly, you are ready to perform a measurement. On the main toolbar click **Go! > Measure!**, or simply click the **Measure** button on the panel on the right hand side of the screen
19. You should see the lamp (heat source) on the optical head light up when a measurement is started. The 'chariot' will then begin to move from one side of the scanner to the other. You will see two lines appear on the main screen of the TCS software: the blue line represents the 'cold' temperature measurements, whilst the red line represents the 'hot' temperature measurements. The red line should form distinct peaks at the position of each body on the stage, which represents the elevated temperature that resulted from the heat input of the optical head (Figure 9).
20. Once the **red line** has clearly passed beyond the last reference standard on the stage, click **Stop**. Once the scan has been stopped, the software will prompt you to **Save** your scan file
21. After the measurement has finished and the file has been saved, the data needs to be processed by the user. This involves **defining the ranges on the axis of measurement** that correspond to each **sample** and **reference standard**. N.B. there will be thermal boundary effects recorded at the edges of each sample and reference standard, which may appear as a spike or a slight curvature in the 'hot' (red)

temperature line. These boundary effects skew the thermal conductivity results and must not be included in the processed data.

22. After the file has been saved, the **Process Data** window will automatically open. By default you first must enter in the ranges for the reference standards (i.e. the first and last bodies on the stage). To do this, click the centre of the white crosshairs and drag them so that the vertical crosshair is sitting at the first position on the standard, which has not been affected by boundary conditions (this takes a judgement call). Then **double click** in the **yellow box** in the 'standards' window that corresponds to the start position of standard 1.
23. Repeat this procedure to set the **end** position of Standard 1. Repeat all of the above for Standard 2. When the positions of the standards have been defined, they will appear as yellow dashed boxes on the scale on the top of the screen. Click **close** on the '**standards'** window when finished.
24. To define the positions of the samples, click the **samples** button on the 'Process data' window
25. Enter the sample name or number in **Sample Name.** Then repeat the procedure (as per the standards) using the crosshairs and the yellow boxes to define the start and end position of each sample. Each time you double click in the **End Position** box, the window will automatically switch to the next sample number for input. If you made a mistake or want to change something, you can manually toggle the sample number using the arrows in the **Sample Number** box. A sample can be deleted by clicking **Del #**.
26. Once all samples have been defined, click **Close** on the **Samples** window.
27. Click **Calculate TC** on the **Process Data** window to complete the calculations.
28. A window called **Statistics** will open when the program has finished performing the calculations. The software keeps the data from all previous scans performed since the program was opened. The bottom most values will be the results from the data you just processed.
29. The data is presented as rows of numbers, which summarise key statistics for each sample. The numbers correspond to the following summary statistics in this order: Mean sample TC (W/m/K); Minimum TC (W/m/K); Maximum TC (W/m/K); G factor (= standard deviation/mean value); and the Inhomogeneity coefficient (= (maximum – minimum)/mean). Also included in the row of values are the sample name, the start and end positions, and the length of the processed segment in mm.
30. Clicking the **Show scan file** button will bring up a window, where the raw data as well as the processed data can be viewed for every individual measurement position (the instrument takes a measurement approximately every mm by default).
31. A graph of the TC profiles of each sample measured can be viewed by clicking the **T.C. (W/m/K)** tab in the top left corner of the viewer window.

Sample Number:	*Arithmetic Mean:*	*Harmonic Mean:*	*Geometric Mean:*
BHDD01 – 01	3.99	3.99	3.99
BHDD01 – 02	4.09	4.07	4.08
BHDD01 – 03	4.12	4.12	4.12
BHDD01 – 04	3.83	3.83	3.83
BHDD01 – 05	3.83	3.83	3.83
BHDD01 – 06	3.94	3.93	3.94
BHDD01 – 07	3.84	3.84	3.84
BHDD01 – 08	3.13	3.08	3.10
BHDD01 – 09	3.78	3.78	3.78
BHDD01 – 10	3.33	3.30	3.31
BHDD01 – 11	3.68	3.67	3.67
BHDD01 – 12	3.80	3.78	3.79
BHDD01 – 13	4.04	4.01	4.03
BHDD01 – 14	3.73	3.73	3.73
BHDD01 – 15	3.81	3.79	3.80
BHDD01 – 16	2.97	2.96	2.96
BHDD01 – 17	2.86	2.85	2.85
BHDD01 – 18	2.93	2.91	2.92
BHDD01 – 19	4.18	4.17	4.18
BHDD01 – 20	2.91	2.90	2.91
BHDD01 – 21	3.09	3.09	3.09
BHDD01 – 22	3.58	3.53	3.56
BHDD01 – 23	2.33	2.33	2.33
BHDD01 – 24	2.27	2.26	2.26
BHDD01 – 25	3.98	3.97	3.98
BHDD01 – 26	4.00	3.99	3.99
BHDD01 – 27	3.36	3.36	3.36
BHDD01 – 28	3.37	3.36	3.36
BHDD01 – 29	2.19	2.18	2.19
BHDD01 – 30	3.37	3.37	3.37
BHDD01 – 31	3.29	3.29	3.29
BHDD01 – 32	3.51	3.51	3.51
BHDD01 – 33	3.11	3.11	3.11
BHDD01 – 34	3.22	3.22	3.22
BHDD01 – 35	3.42	3.41	3.42
BHDD01 – 36	3.55	3.55	3.55
BHDD01 – 37	3.35	3.34	3.35
BHDD01 – 38	2.75	2.71	2.73
BHDD01 – 39	3.62	3.61	3.61
BHDD01 – 40	3.83	3.82	3.83
BHDD01 – 41	3.76	3.75	3.75

Table A1: Calculated Arithmetic, Harmonic & Geometric Means for hole BHDD01

Sample Number:	*Arithmetic Mean:*	*Harmonic Mean:*	*Geometric Mean:*
PHDD1202 – 01	2.85	2.84	2.85
PHDD1202 – 02	2.77	2.77	2.77
PHDD1202 – 03	2.35	2.34	2.35
PHDD1202 – 05	2.46	2.32	2.39
PHDD1202 – 06	2.19	2.17	2.18
PHDD1202 – 07	2.96	2.94	2.95
PHDD1202 – 08	2.63	2.55	2.59
PHDD1202 – 09	2.50	2.48	2.49
PHDD1202 – 12	2.41	2.40	2.41
PHDD1202 – 13	2.54	2.54	2.54
PHDD1202 – 15	2.31	2.31	2.31
PHDD1202 – 16	2.58	2.57	2.57
PHDD1202 – 18	2.23	2.22	2.23
PHDD1202 – 19	2.51	2.51	2.51
PHDD1202 – 20	2.34	2.34	2.34
PHDD1202 – 21	2.74	2.74	2.74

Table A2: Calculated Arithmetic, Harmonic & Geometric Means for hole PHDD1202

Sample Number:	*Arithmetic Mean:*	*Harmonic Mean:*	*Geometric Mean:*
SDDD01 – 01	2.66	2.65	2.66
SDDD01 – 03	2.90	2.82	2.86
SDDD01 – 06	2.93	2.91	2.92
SDDD01 – 08	2.96	2.95	2.96
SDDD01 – 09	2.61	2.61	2.61
SDDD01 – 11	2.64	2.63	2.64
SDDD01 – 12	2.45	2.45	2.45
SDDD01 – 14	2.96	2.93	2.95
SDDD01 – 15	3.04	3.01	3.03
SDDD01 – 17	3.37	3.36	3.36
SDDD01 – 18	2.77	2.75	2.76
SDDD01 – 20	2.19	2.18	2.19
SDDD01 – 21	2.78	2.75	2.76
SDDD01 – 22	2.53	2.34	2.43
SDDD01 – 23	3.51	3.49	3.50
SDDD01 – 24	3.39	3.39	3.39
SDDD01 – 25	4.12	4.12	4.12
SDDD01 – 26	3.31	3.31	3.31
SDDD01 – 27	3.21	3.20	3.21
SDDD01 – 28	2.30	2.30	2.30
SDDD01 – 29	2.52	2.51	2.51
SDDD01 – 30	2.73	2.73	2.73
SDDD01 – 31	2.27	2.26	2.26
SDDD01 – 32	2.36	2.36	2.36

Table A3: Calculated Arithmetic, Harmonic & Geometric Means for hole SDDD01

Stratigraphic Logging of Cores:

SAMPLE # & DEPTH:	**BHDD01** DESCRIPTION:	AVERAGE GRAIN SIZE:
237.82 #1	SEDIMENTARY – SANDSTONE: • Clasts of quartz approximately 1mm in size contained within brown matrix. Occasional clast up to 5mm in size • No bedding or foliation observed	1mm
242.40 #2	SEDIMENTARY – SANDSTONE: • Predominantly clasts of quartz of approximately 1mm in size contained within very fine-grained brown matrix. • No bedding or foliation observed but quartz vein rins through sample (2-3mm thick)	1mm
246.95 #3	SEDIMENTARY – CONGLOMERATE: • Very coarse → gravel sized grains ranging in sizes from 1mm (Quartz), 5mm (Fdsp) to >1-2cm clasts. • No bedding or foliation observed – clasts are poorly sorted within fine grey matrix.	9mm
252.78 #4	SEDIMENTARY – DEFORMED SHALE • Very fine grained silts still with some <5mm grains of Quartz from previous rock types. • Layering not seen due to large amount of deformation • Fractures present along length of sample	<0.1mm
260.58 #5	SEDIMENTARY – SHALE: • Very fine grained silts alternating from light to dark grey. • Layer present – approximately 1mm alternating light and dark layers. • Layering perpendicular to up direction.	<0.1mm
266.91 #6	SEDIMENTARY – SHALE: • Very fine grained light and dark silts • Dark bands more prominent in this sample than last (#5) • Layering present – up to 1mm thick • Layering perpendicular to up direction	<0.1mm
273.71 #7	SEDIMENTARY – SHALE: • Very fine grained light and dark silts • Dark bands still more prominent – up to 2mm thick • Layering present perpendicular to up direction	<0.1mm
280.03 #8	SEDIMENTARY – SANDSTONE: • Predominantly quartz clasts <1mm in size, approximately 0.5mm. Occasional feldspar clasts up to 1mm in size. • Less evidence for brown matrix in this sample • No bedding or foliation present	0.5mm
287.42 #9	SEDIMENTARY – SHALE: • Very fine grained light and dark grey material	<0.1mm

	• Layering present perpendicular to up direction • Some layers deformed and curved.	
294.90 #10	SEDIMENTARY - SHALE: • Very fine grained light and dark grey silt. • Layering predominantly light coloured with layers thinning to approximately 0.5mm • Layers perpendicular to upward direction	<0.1mm
300.21 #11	SEDIMENTARY – SANDSTONE/MUDSTONE • Fine grained quartzed <1mm in size within very fine brown matrix. • Occasional larger clasts of qtz/fdsp approximately 1-2mm in size • No layering or bedding present.	0.5mm
303.77 #12	SEDIMENTARY – MUDSTONE: • Fine grained <1mm quartz clasts held within fine brown mud matrix. • No larger clasts present. • No layering or bedding present.	<0.1mm
304.93 #13	SEDIMENTARY – MUDSTONE: • Fine grained clasts <1mm with occasional larger qtz/fdsp clasts of approximately 1mm in size. • Very fine grained brown matrix • No layering or bedding present.	<0.1mm
313.68 #14	SEDIMENTARY – CONGLOMERATE (SANDSTONE): • Very coarse to gravel sized quartz grains ranging from 2mm to 2cm. • Clasts held within fine brown matrix (sandstone properties occuring upwards) • Poorly sorted larger grains ranging from 0.5 to 2cm in size. • No bedding or foliation present.	9mm
320.62 #15	SEDIMENTARY – FINER TO COARSE SANDSTONE: • Finer (1mm) quartz grains coarsening upwards to coarse (5-7mm) quartz grains held within fine brown-purple matrix. • No layering or bedding evident.	4mm
331.31 #16	SEDIMENTARY – COARSE SANDSTONE: • Same as coarse sandstone in last sample (#15) • Grains ranging from 1-5/6mm • No layering or bedding present	3mm
341.21 #17	SEDIMENTARY – SANDSTONE: • Very coarse quartz grains 1-6mm, feldspar grains approximately 2mm • Some type of alteration product (white, fine) present also. • Large growths of quartz present in this sample • No bedding or foliation present.	3mm
346.96 #18	SEDIMENTARY - SANDSTONE/CONGLOMERATE: • Quartz grains coarsening upwards from 1-2mm to approximately 4mm.	2mm

	• Clasts contained within very fine grained brown matrix • No bedding or foliation present.	
355.94 #19	SEDIMENTARY – SANDSTONE/CONGLOMERATE: • Coarse (>2mm) quartz grains with occasional 0.5cm clasts. • Fine white material present (alteration) as well as fine brown matrix No bedding or foliation present	4mm
361.39 #20	SEDIMENTARY – MUDSTONE/FINE->COARSE SAND: • Fine (<1mm) quartz grains within muddy matrix coarsening upwards to 1-3mm crystallised grains of quartz with less brown matrix and more fdsp grains up to 1mm. • No bedding or foliation present.	1mm
373.38 #21	SEDIMENTARY – SANDSTONE: • Fine quartz and micas (fluid flow?) less than 1mm coarsening upward to quartz clasts of approximately 2-3mm in size within fine brown/purple matrix. • No bedding or foliation present.	0.7mm
378.30 #22	SEDIMENTARY – SANDSTONE: • Quartz clasts on average 1mm in size with occasional clasts up to 3mm Some qtz/fdsp clasts at top of sample, approximately 2mm. • Contained within fine brown matrix • No bedding or foliation present.	1mm
396.58 #23	SEDIMENTARY – SANDSTONE: • Quart grains 0.5mm in size. More matrix dominated with evident fractures and regions of probable fluid flow. • Quartz in fluid regions up to 1mm. • No bedding or foliation present.	0.5mm
390.93 #24	SEDIMENTARY – SANDSTONE: • Quartz grains range from 0.5 – 1mm in size. • Some regions of possible fluid flow present in this sample too – include fine (0.2mm) grained micas • No bedding or foliation present	0.7mm
398.17 #25	SEDIMENTARY – SANDSTONE: • Quartz approx. 0.5mm - 1mm average grain size • No bedding or foliation present.	0.7mm
405.30 #26	SEDIMENTARY – SANDSTONE: • Quartz approx. 0.5mm average grain size • Fine brown matrix dominated • No bedding or foliation present	0.5mm
412.09 #27	SEDIMENTARY – SANDSTONE: • Average grain size 0.5mm up to 1mm • Fine brown matrix not as dominant • No bedding or foliation present.	0.7mm
420.74	SEDIMENTARY – SANDSTONE: • Average grain size 0.4mm, occasional grains larger up	0.4mm

#28	to 1mm. • Grains more interspersed within fine brown matrix. • No bedding or foliation present.	
427.51 #29	SEDIMNETARY – SANDSTONE: • Average grain size approx. 1mm • Parts largely matrix dominated, other parts lacking matrix. • From size of core sample possible foliations present. • Occasional large clasts of almost pure matrix	1mm
435.25 #30	SEDIMENTARY – FINE GRAINED SANDSTONE: • Average grain size 0.5mm • Matrix dominated – brown colour of core • No bedding or foliation present	0.5mm
441.60 #31	SEDIMENTARY – SANDSTONE: • Average grain size 1-1.5mm • Becoming matrix dominated near top of sample with smaller quartz grains (<0.5mm) • No bedding or foliation present.	1.2mm
451.83 #32	SEDIMENTARY – SANDSTONE: • Grain sizes average 0.5mm some interspersed up to 1mm • Fine brown matrix present but not dominating. • No bedding or foliation present.	0.7mm
460.84 #33	SEDIMENTARY – SANDSTONE: • Grain sizes up to and average 1mm – band in middle of specimen may be up to 2mm. • Fine brown matrix dominating • No bedding or foliation present.	1mm
469.39 #34	SEDIMENTARY – SANDSTONE: • Coarser sandstone, grains averaging 1.5-2mm with occasional large clasts. • Matrix dominated band at top of core • No bedding or foliation present	1.7mm
469.60 #35	SEDIMENTARY – SANDSTONE: • Finer grained, grains averaging 0.5mm • Fine brown matrix evident, but not dominating • No bedding or foliation present.	0.5mm
482.17 #36	SEDIMENTARY – SANDSTONE: • Finer grains, averaging 0.5mm • Abundant quartz • No bedding or foliation present	0.5mm
492.01 #37	SEDIMENTARY – SANDSTONE: • Finer grains, averaging 0.5mm • Abundant quartz • No bedding or foliation present	0.5mm
504.78 #38	SEDIMENTARY – SANDSTONE: • Grains ranging in size from 2mm (bottom of sample) to 0.5mm fining upward in sample • Average grain size approx. 0.7mm • Layering present in form of varying thickness	0.7mm

	• Foliation present.	
514.71 #39	SEDIMENTARY – SANDSTONE/CONGLOMERATE • Grains average 0.5-1mm in size • Matrix (very fine) is dominating in some parts • Clusters of fdsp grains w qtz give conglomerate appearance • Possible banding of dark material through middle of specimen.	0.7mm
535.51 #40	GAWLER RANGE VOLCANICS: • Large clusters of grains <1mm with fine brown matrix • Occasional grains up to 4mm • Takes on conglomerate-type texture • No bedding or foliation present.	1mm
541.14 #41	GAWLER RANGE VOLCANICS: • Extremely large grains,, easily averaging 3-4mm, up to 1cm • Matrix not as dominant, grain dominated • Poorly sorted grains • No bedding or foliation present.	3.5mm

Table A4: Stratigraphic logging of core for hole BHDD01

SAMPLE # & DEPTH(m):	**PHDD1202** DESCRIPTION:	AVERAGE GRAIN SIZE:
904 #1	SEDIMENTARY – SANDSTONE: • Large range of grain sizes ranging from 0.5mm to almost 2cm (lithic fragments) • Average grain size 5mm – but largely varying • No bedding or foliation present	5mm
905.60 #2	SEDIMENTARY – MUDSTONE: • Average grain size very fine with occasional lithic fragments up to 5mm in size • Mostly muddy matrix dominated (<0.1mm) • No bedding or foliation present	0.5mm
909.50 #3	IGNEOUS – VOLCANICS: • Medium grained average size 1mm • Contains qtz and fdsp • Fractures infilled with dark fine grained material	1mm
945.50 #5	METASEDS – SKARN: • Deformed, qtz veins prominent throughout • Grain size greatly varies from <1mm qtz to large cm scale lithic fragments	1mm
951.9 #6	METASEDS – SKARN: • Highly deformed, some inclusions of possible alteration? • Grain size ranges from 0.5mm to 8/9mm • Occasional larger 1cm fragments	3mm
967.22 #7	METASEDS – SKARN: • Highly deformed, possible fluid flow • Grain size ranges from very fine (<0.1mm) up to 1mm – average 0.2mm – very fine	0.2mm
980.09 #8	METASEDS – SKARN: • Highly deformed – possible fluid flow through fractures • Not as many qtz veins • Grains range from 0.5mm – 1mm in size	0.7mm
984.60 #9	METASEDS – SKARN: • Deformed, possible fluid flow, no quartz veins present • Average grain size 1mm	1mm
1006.98 #12	METASEDS – SKARN: • Appears less deformed, no evidence for alteration or fluid flow. • Average grain size 0.5-1mm	0.7mm
1014.16	METASEDS – SKARN:	1mm

#15	• Deformed, qtz veins present • Blotchy patches all over core – alteration? • Average grain size approx. 1mm	
1025.16 #15	METASEDS – SKARN: • Not as deformed, possible thin qtz vein • Qtz rich, grains approx. 1mm in size – visible • Occasional includiond of darker coloured grains – inclusions up to 1cm in size	1mm
1040.41 #16	METASEDS – SKARN: • Highly deformed – thick quartz veins present • Average grain size approx. 1mm • Quite a lot of fdsp in this sample	1mm
1053.09 #18	METASEDS – SKARN: • Deformed, thick quartz veins present • 1mm light coloured grains spotted through sample • Very fine (<0.5mm) grains interspersed with 1mm light coloured grains.	0.7mm
1059.60 #19	METASEDS - SKARN: • Highly deformed, thin quartz veins present • Large >2cm sized inclusions filled with very fine grained grey material • Average grain size <0.5mm – not visible	0.1mm
1068.36 #20	METASEDS – SKARN: • Highly deformed, abundant quartz veins present • Stretching of grey coloured inclusions and grains – deformation • Grains very fine (<0.5mm) – not visible	0.1mm
1072.37 #21	METASEDS – SKARN: • Deformed, 1 thick and a few thin quartz veins • Possible banding/layering • Average grain size approx. 1mm	1mm

Table A5: Stratigraphic logging of hole PHDD1202

SAMPLE # & DEPTH(m):	**SDDD01** DESCRIPTION:	AVERAGE GRAIN SIZE:
262.68 #32	SEDIMENTARY – ARKOSIC SANDSTONE: • Grains well sorted • Average grain size 1mm • No bedding or foliation present	1mm
268.94 #31	SEDIMENTARY – ARKOSIC SANDSTONE: • Grains well sorted • On average slightly larger grains evident but average size still 1mm • No bedding or foliation present although some layering of larger grains	1mm
276.61 #30	SEDIMENTARY – ARKOSIC SANDSTONE: • Grains well sorted • Average grain size 1mm • No bedding or foliation present	1mm
299.57 #29	SEDIMENTARY – ARKOSIC SANDSTONE: • Grains well sorted with occasional large lithic fragments up to 1cm • Start of banding of lighter coloured sandstone at top of sample • Average grain size 1mm • No bedding or foliation present	1mm
299.76 #28	SEDIMENTARY – ARKOSIC SANDSTONE: • Thick banding (>10cm) of light then dark sandstone • Grains in light average 0.5mm, grains in dark average 0.5-1mm • No bedding or foliation present	0.7mm
310.83 #27	SEDIMENTARY – ARKOSIC SANDSTONE: • Grains well sorted • Average grains size 1mm • Some larger (2mm) fdsp grains • No bedding or foliation present	1mm
318.17 #26	SEDIMENTARY – ARKOSIC SANDSTONE: • More grain dominated • Average grain size 2mm with quite a lot of feldspar • No bedding or foliation present	2mm
321.71 #25	SEDIMENTARY – ARKOSIC SANDSTONE: • Grain dominated • Average grain size 1mm up to 2-3mm in some fdsp clasts • Odd 1cm clasts dispersed throughout sample • No bedding or foliation present	1mm
326.20 #24	SEDIMENTARY – ARKOSIC SANDSTONE: • Very coarse grained – average 3mm in size but some smaller 1mm grains • Grain dominated but still molded in very fine grains brown matrix • No bedding or foliation present	3mm
328.00	SEDIMENTARY – ARKOSIC SANDSTONE:	4mm

#23	• Similar to sample 24 but with larger grain size – almost conglomerate texture • Average grain size 4mm (qtz) up to 1cm • Brown material very fine grained present between grains • No bedding or foliation present	
329.77 #22	MAFIC DYKE – DOLERITE: • Extremely vine grained brown material • Qtz vein present – apprx 5mm thick • No bedding or foliation present	0.1mm
332.03 #21	MAFIC DYKE – DOLERITE: • Extremely fine grained brown material • Qtz vein present approx. 2mm thick • No bedding or foliation present	0.1mm
341.43 #20	MAFIC DYKE – DOLERITE: • Very fine grained dark grey to reddy brown material • Many fractures infilled by fine white material • Small grains (0.8mm) of amphibole(?) present • No bedding or foliation present	0.1mm
347.48 #18	MAFIC DYKE – DOLERITE: • Very fine grained dark grey material with 0.8mm grains of amphibole (?) common throughout sample • 2 fractures with fine white material infilled • No bedding or foliation present	0.1mm
378.40 #14	GRANITE: • Very coarse grained granite with 2mm-4mm biotite grains, 102cm fdsp grains and 2mm qtz grains • Average grain size 7mm • No bedding or foliation present	7mm
400.7 #12	MAFIC DYKE – DOLERITE: • Dark grey material composed of 0.5mm grains of amphibole. • Some grains up to 7-8mm – not common. • No bedding or foliation present	0.5mm
409.67 #11	MAFIC DYKE – DOLERITE: • Dark grey material composed of 0.5mm grains of amphibole(?) • No bedding or foliation present	0.5mm
420.58 #09	MAFIC DYKE – DOLERITE: • Dark grey material composed of 0.5mm grains of amphibole(?) • No bedding or foliation present	0.5mm
429.32 #08	MAFIC DYKE – DOLERITE: • Dark grey material composed of 0.5mm grains of amphibole (?) • No bedding or foliation present • Fine fractures approx. 0.8mm with fine white material infill. • No bedding or foliation present	0.5mm
440.24	GRANITE:	10mm

#06	• Very coarse grain granite, with 2mm biotie, 3/4mm qtz grains and 1-3.5cm fdsp grains • Average grain size 1cm • No bedding or foliation present	
445.76 #03	GRANITE: • Some qtz and biotite as sample 6 but fdsp up to 10cm – dominates entire sample • Occasional 3mm micas present • No bedding or foliation present	70mm

Table A6: Stratigraphic logging of hole SDDD01

The following figures are representative of the figures and images that were produced and are available for every core sample within this data set. Due to file size restrictions, not all 85 samples' worth of figures could be included in the appendix, however the following figures give an example of the data analysis and figures produced for each sample.

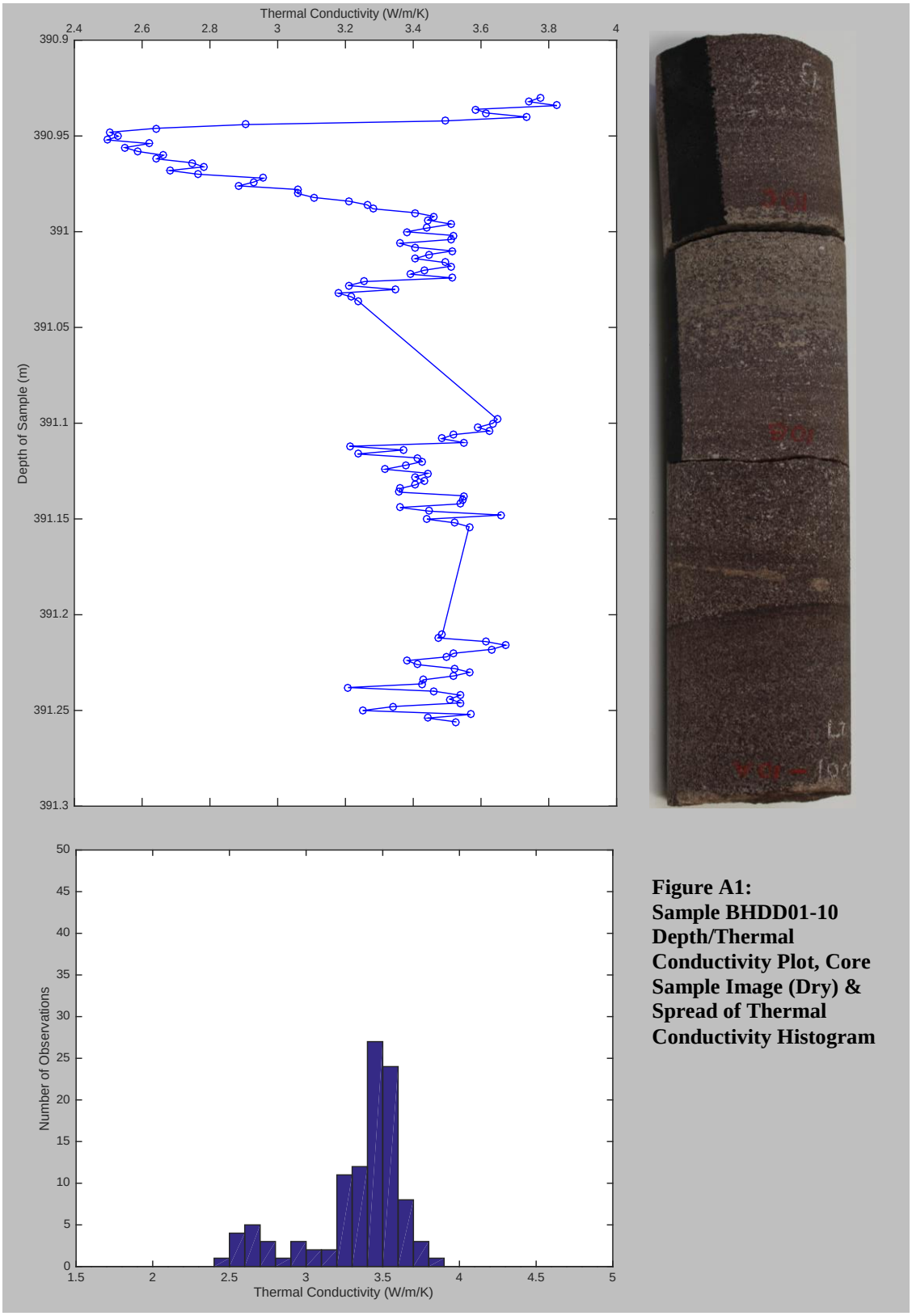

Figure A1: Sample BHDD01-10 Depth/Thermal Conductivity Plot, Core Sample Image (Dry) & Spread of Thermal Conductivity Histogram

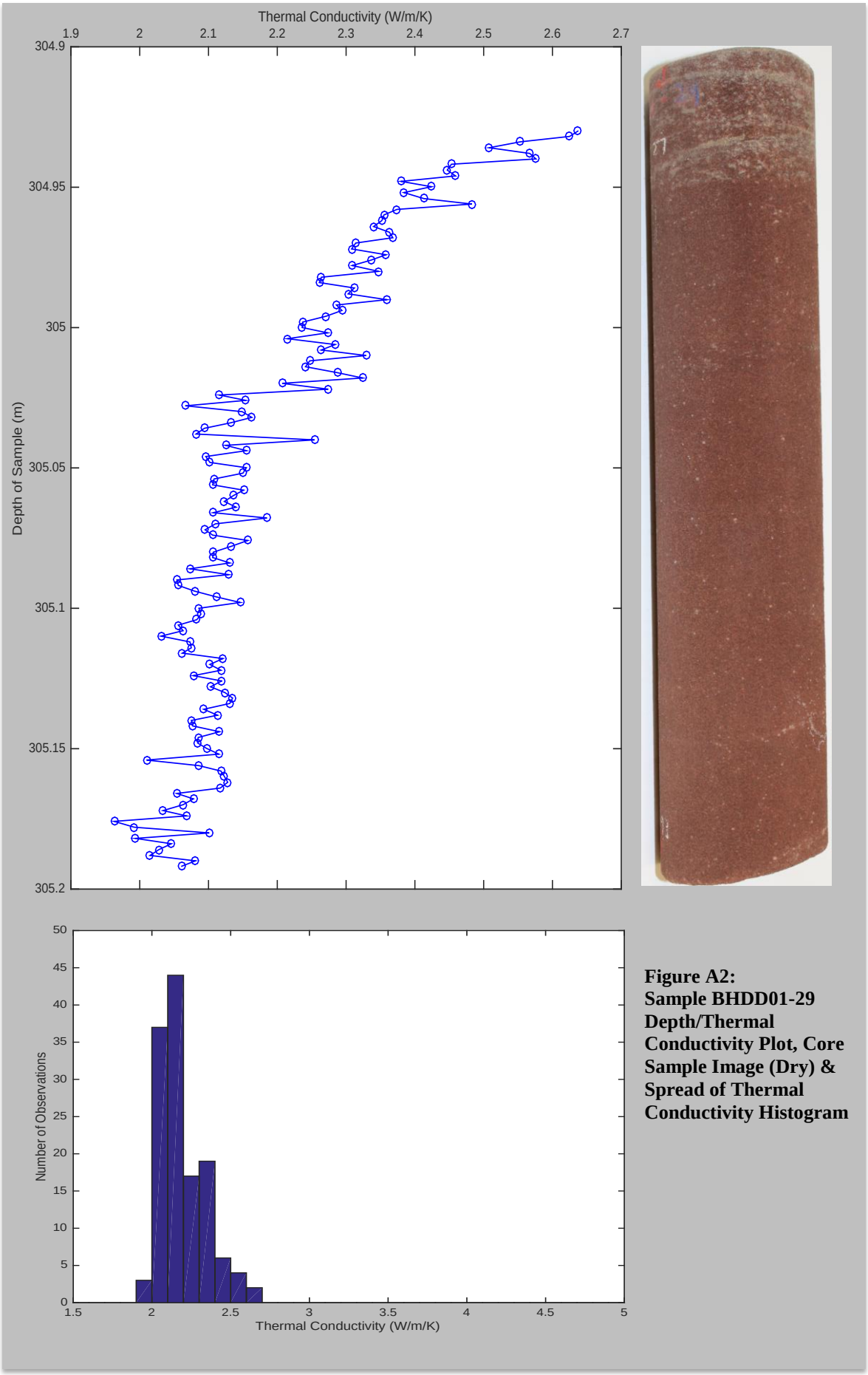

Figure A2:
Sample BHDD01-29 Depth/Thermal Conductivity Plot, Core Sample Image (Dry) & Spread of Thermal Conductivity Histogram

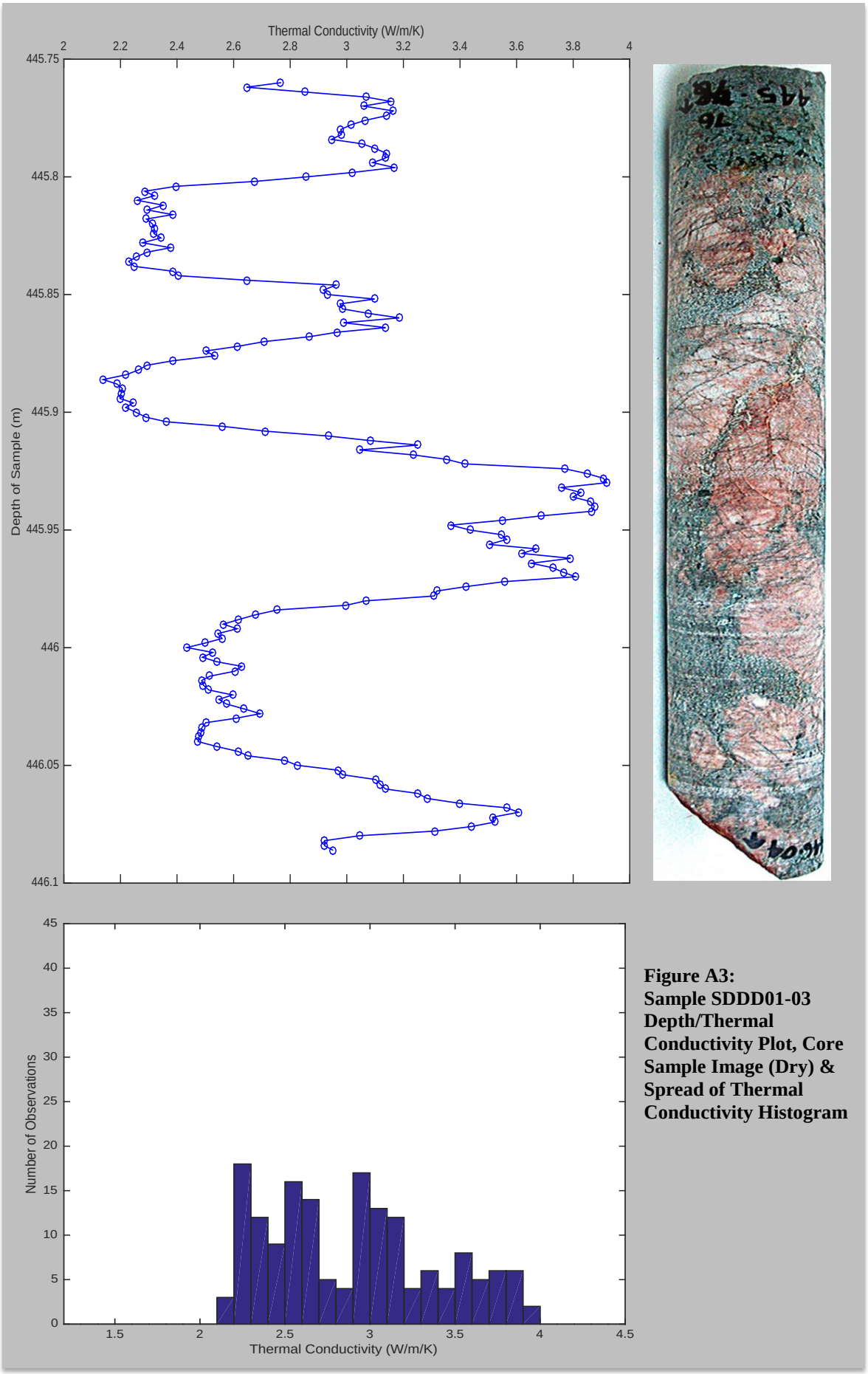

Figure A3:
Sample SDDD01-03 Depth/Thermal Conductivity Plot, Core Sample Image (Dry) & Spread of Thermal Conductivity Histogram

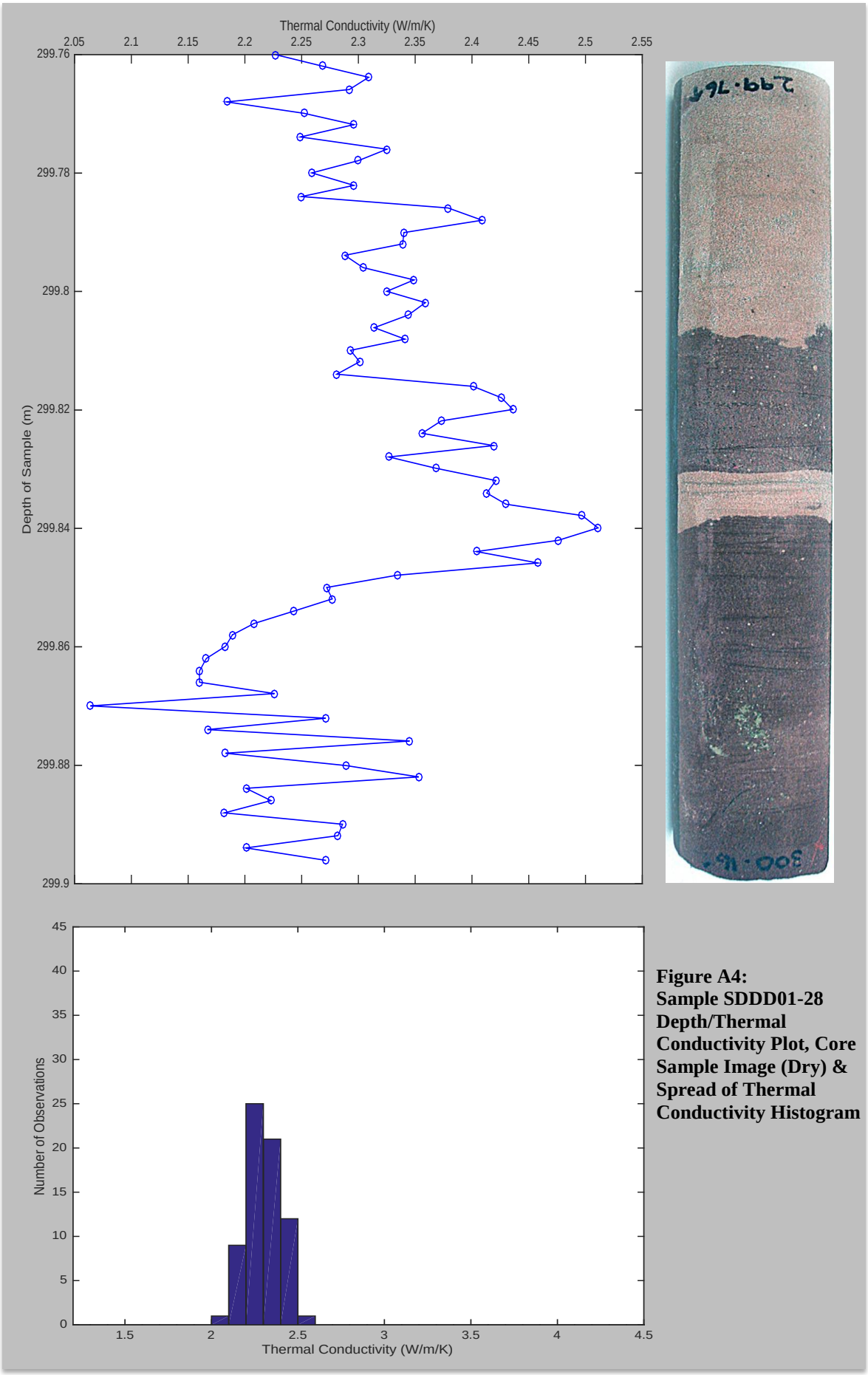

Figure A4:
Sample SDDD01-28 Depth/Thermal Conductivity Plot, Core Sample Image (Dry) & Spread of Thermal Conductivity Histogram

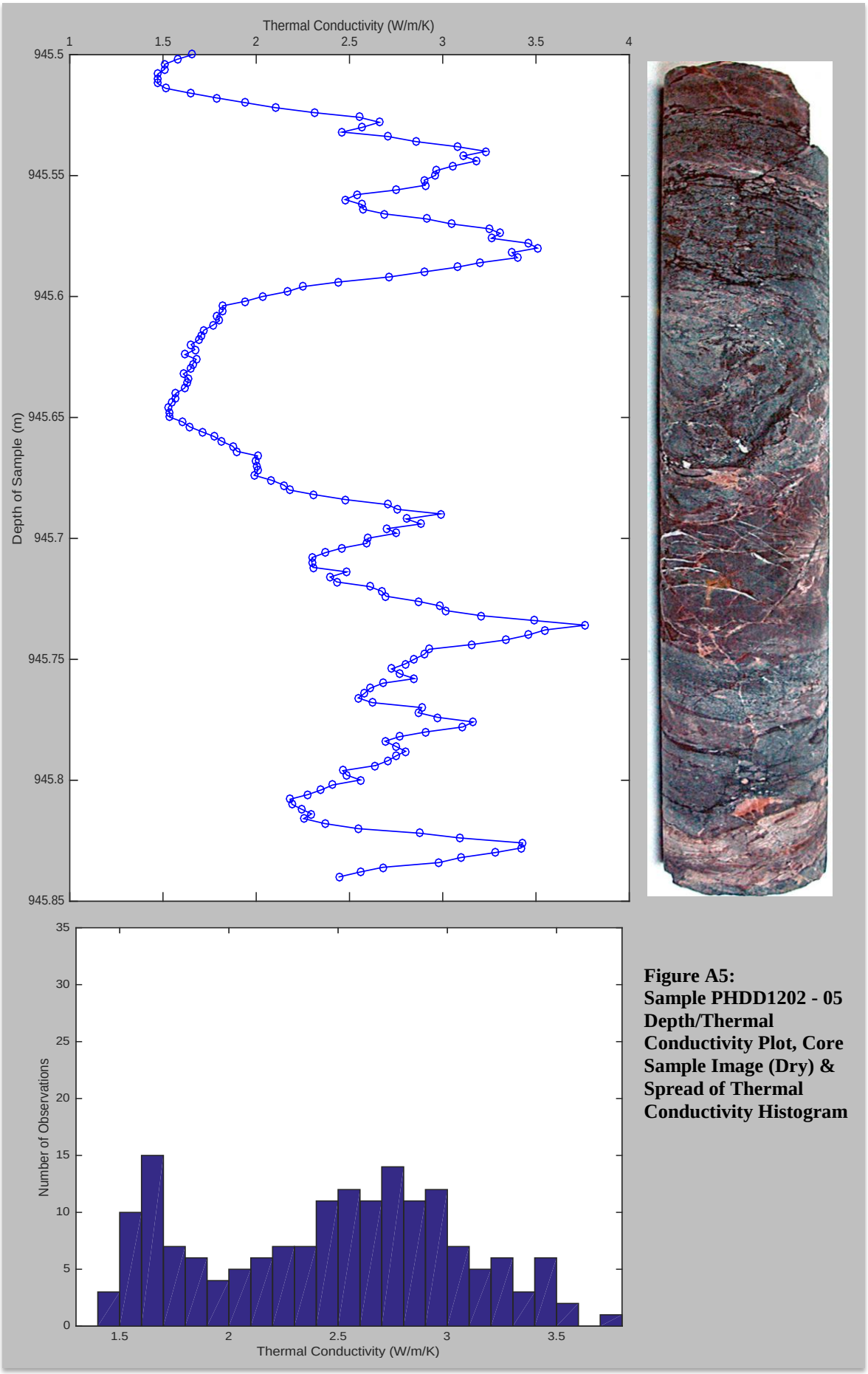

Figure A5:
Sample PHDD1202 - 05 Depth/Thermal Conductivity Plot, Core Sample Image (Dry) & Spread of Thermal Conductivity Histogram

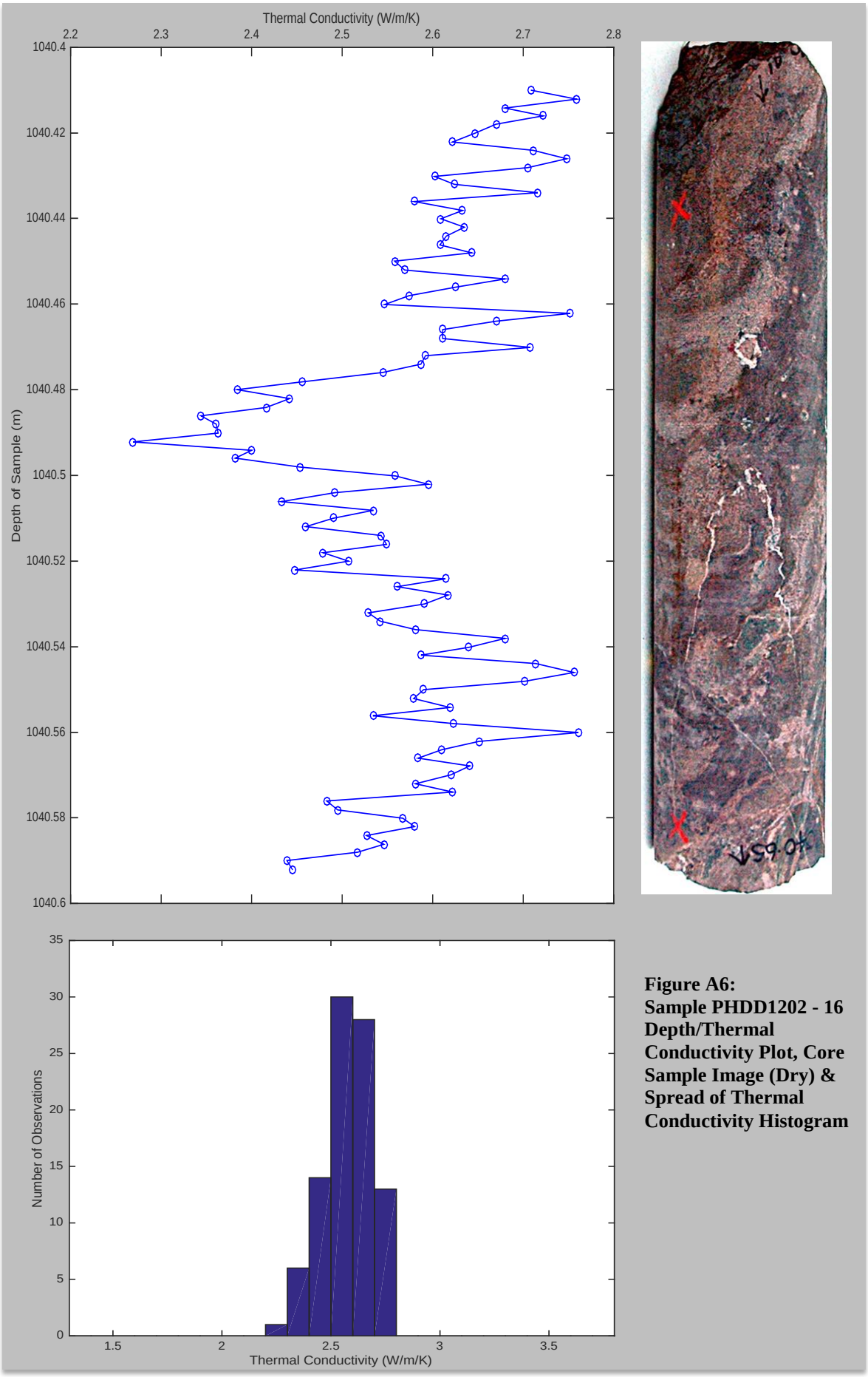

Figure A6:
Sample PHDD1202 - 16 Depth/Thermal Conductivity Plot, Core Sample Image (Dry) & Spread of Thermal Conductivity Histogram